the *YB-1* genomic sequence in the targeting vector to allow for positive and negative selection of DNA when introduced into ES cells.[24] The targeting construct was linearized at a unique *Not*I site located on the plasmid vector.

Isolation of heterozygous mutant embryonic stem cell lines. The ES cell line CCE was cultured on a feeder cell layer and electroporated, using 5×10^7 cells and 50 μg of the linearized targeting vector DNA, as described.[25] The transfected cells were subjected to positive and negative selection, using G418 (250 μg/ml; Geneticin, GIBCO/BRL) and ganciclovir (GANC) (5 m*M*; a gift of Nihon Syntex) as selective agents. Colonies doubly resistant to G418 and GANC were grown on 24-well plates to expand them for Southern blot analysis. DNA was isolated from each cell line and analyzed by Southern blot hybridization.

Southern blot analysis. Genomic DNA (8 μg) was digested with *Eco*RV and *Bgl*II, then run on a 0.7% agarose gel and transferred to a nylon membrane filter (Hybond N1; Amersham). The filter was hybridized with a 0.3-kb *Eco*RV/*Eco*RI fragment (5′ internal probe A) and a 0.3-kb *Xho*I/*Hin*dIII fragment (3′ flanking probe B), labeled with [α-^{32}P]dCTP. The membrane was washed, applied to an imaging plate, and analyzed using a Bio-image analyzer BAS 2000 (Fuji Photo Film Co., Kanagawa).

RNA isolation and northern blot analysis. Cells in the exponential growth phase were transferred to a medium without feeder layer cells and further cultured on a gelatin-coated dish for 4 days to avoid contamination with *YB-1* mRNA derived from feeder cells. Total RNA was isolated using an RNeasy spin column (Qiagen, Hilden, Germany). RNA samples (10 μg/lane) were separated on a 1% formaldehyde-agarose gel and were transferred to a membrane. The membranes were hybridized with ^{32}P-labeled mouse YB-1 1.2-kb cDNA as a probe.[15] Radioactivity was visualized by autoradiography and was analyzed using a Fujix Bas 2000 bioimaging analyzer (Fuji Photo Film Co., Tokyo).

Immunoblotting of the YB-1 protein. The cells were lysed in TNE buffer (50 m*M* Tris-HCl (pH 7.5), 150 m*M* NaCl, 1 m*M* EDTA, 0.5% NP-40, 1 m*M* PMSF, 10 μg/ml leupeptin, 10 μg/ml aprotinin), and boiled in western sample buffer for 10.0% SDS-PAGE and western blot analysis. An antibody to YB-1 was generated as described previously.[15] PCNA-specific antibody (PC10; Santa Cruz) and p21 (sc-817; Santa Cruz) were used for western blotting.

Proliferation rates. To determine the proliferation rates of ES cells, 5×10^5 cells were plated in triplicate in 6-well plates and the cell numbers were determined at the indicated time points using a CASYR cell counter.

Clonogenic survival assay. ES cells were plated on gelatin-coated 6-well plates at a density of approximately 500 cells/well. Twenty-four hours after plating, ES cells were treated with various chemical agents, X-rays or UV irradiation. Plates were incubated for 7 days and the surviving ES cell colonies in each well were counted after staining with Giemsa. The plating efficiency was ~60–80%. The relative sensitivity of each clone of *YB-1*$^{+/-}$ ES cells was determined by dividing the IC_{90} value for each cell line by that of wild-type (*YB-1*$^{+/+}$) ES cells.

MTS survival assay. CellTiter 96 Aqueous One Solution cell proliferation Assay (Promega) was used to evaluate drug sensitivities. The 96-well plates were inoculated with 4000 cells/well in a volume of 100 μl of ES medium. Twenty-four hours later, drugs were added at various concentrations. Seventy-two hours later, 20 μl of MTS/PES was added, and incubation was continued for 2 h at 37°C. In the presence of the electron-coupling reagent PES, MTS is reduced by dehydrogenase enzymes found in metabolically active cells into a formazan product that is readily soluble in tissue culture medium. The quantity of formazan product was measured in terms of the absorbance at 490 nm. At least five different drug concentrations were used to determine the IC_{50} values, and each drug concentration was replicated in 4 wells for each individual experiment. The relative sensitivity of each *YB-1*$^{+/-}$ ES cell clone was determined by dividing the IC_{50} value for each cell line by the *YB-1*$^{+/+}$ ES cell line IC_{50} value.

Results

Targeted disruption of the *YB-1* gene. The mouse *YB-1* gene, which encodes a 49-kDa protein, is composed of 8 exons, spans more than 16 kb, and is 99% identical to human YB-1. A region of genomic DNA carrying part of two exons and the adjacent intron region, was replaced by a *neo* cassette (Fig. 1A). This region was chosen as the target since it encodes the C-terminal domain of the YB-1 protein, which is essential for protein interaction and nucleoside binding.[26] The resulting construct was electroporated into ES cells, and cells showing increased resistance to both G418 and GANC were selected. The DNAs of resistant clones were digested with restriction enzymes and hybridized with several different probes. Homologous recombinants were characterized by the appearance of a 5.5-kb *Eco*RV fragment with the 5′-internal probe A, and a 10.3-kb *Bgl*II fragment with the 3′-flanking probe B (Fig. 1, B and C). Additional Southern blot analysis using other restriction enzymes confirmed the targeted disruption of one allele of *mouse YB-1* (data not shown). Furthermore, hybridization with the *neo* probe showed that the predicted genomic DNA fragment size is similar in all of these clones. Approximately 4% of G418- and GANC-doubly resistant cells carried the expected structure for the mutated allele.

Decrease in mRNA expression and protein levels in heterozygous *YB-1*$^{+/-}$ ES cells. Northern blot analysis of YB-1 mRNA, using the full-length YB-1 cDNA as a probe, was performed in *YB-1*$^{+/+}$ cells and three different clones of *YB-1*$^{+/-}$ cells. We found that *YB-1*$^{+/-}$ cells contain approximately half the amount of mRNA detected in *YB-1*$^{+/+}$ cells (Fig. 2A). Consistent with this observation, western blot analysis of heterozygously disrupted mutant cells also showed a reduction in YB-1 protein levels. For semi-quantitative analysis, various amounts of cell lysate were applied to the same gel, and we estimated that the protein level of *YB-1*$^{+/-}$ cells was reduced to approximately 50–60% of the wild-type level (Fig. 2B). *YB-1*$^{+/-}$ cells thus established grew normally in ES medium, despite these characteristics. The doubling time of *YB-1*$^{+/+}$ and three clones (1, 2, and 5) of *YB-1*$^{+/-}$ cells were 10.2, 10.0, 9.0, and 10.2 h, respectively (Table 1). Thus, no apparent growth retardation or abnormal cell morphology was found in *YB-1*$^{+/-}$ cells, in spite of the reduced content of YB-1 protein.

Drug, X-ray, and UV irradiation sensitivity of targeted cells to DNA damaging agents. YB-1 has been proposed to be involved in the sensitivity of cells to DNA-damaging agents such as cisplatin and mitomycin C.[15] We therefore explored the role of YB-1 heterozygosity in sensitizing ES cells to a variety of cytotoxic agents using both MTS and clonogenic survival assays. As shown in Table 2, we found that *YB-1*$^{+/-}$ cells are more sensitive to cisplatin and mitomycin C, and moderately more sensitive to etoposide than *YB-1*$^{+/+}$ cells. This enhanced sensitivity was seen in three independently isolated *YB-1*$^{+/-}$ clones (1, 2, and 5), and the depletion of YB-1 was required for drug sensitization. Comparisons made at the IC_{50} dose for cisplatin revealed that *YB-1*$^{+/-}$ cells were approximately 3-fold more sensitive to cisplatin than *YB-1*$^{+/+}$ cells (IC_{50}=20.0 μ*M*). Similarly, comparisons made at the IC_{50} dose for mitomycin C revealed that *YB-1*$^{+/-}$ cells were approximately 5-fold more sensitive to mitomycin C than *YB-1*$^{+/+}$ cells (IC_{50}=9.0 μ*M*). Also, comparisons made at the IC_{50} dose for etoposide revealed that *YB-1*$^{+/-}$ cells showed a moderate level of sensitivity (1.4-

fold), compared with *YB-1*$^{+/+}$ cells (IC_{50}=0.6 μ*M*) (Table 2A). Taken together, the results described above suggest that the concentration of YB-1 appears to correlate inversely with cellular sensitivity to DNA-damaging agents. Clonogenic survival assays were also performed on *YB-1*$^{+/+}$ and *YB-1*$^{+/-}$ cells to determine whether differences observed in MTS survival assays would translate into differences in clonogenicity. We treated cells with a variety of chemotherapeutic drugs, X-ray or UV irradiation and then incubated them for 7 days before counting colonies with greater than 50 cells per colony. This assay provides a longer-term assessment of cell growth than the MTS assay and directly assesses the ability of individual cells to proliferate into viable colonies. We tested the cytotoxicity of cisplatin, mitomycin C, etoposide, X-rays, and UV irradiation against *YB-1*$^{+/+}$ and *YB-1*$^{+/-}$ cells. The dose of agent required to reduce colony formation to 10% (IC_{90}) of that by the control non-treated cells is shown in Table 2B. Consistent with data gained in MTS assays and previous observations in KB cells,[15] *YB-1*$^{+/-}$ cells exhibited greater sensitivity to cisplatin and mitomycin C than *YB-1*$^{+/+}$ cells. The dose-modifying factor for equivalent cell killing (IC_{90}) was approximately 2.0-fold for cisplatin and mitomycin C. In contrast, *YB-1*$^{+/-}$ cells were found to be as sensitive as *YB-1*$^{+/+}$ cells to etoposide, X-ray and UV irradiation (Table 2B, Fig. 3). Our results suggested that the reduction of YB-1 level in ES cells preferentially enhances their sensitivity to DNA cross-linking agents.

No change of p21 levels between YB-1$^{+/+}$ and YB-1$^{+/-}$ cells. Swamynathan *et al.* established DT40 cells, in which one allele of Chk-YB-1b is disrupted.[27] The DT40YB1b (+/−) cells showed multiple abnormalities, such as slow growth rate, increased cell size, increased genomic DNA content, and reduced p21 levels.[27] We found no apparent growth retardation or abnormal cell morphology in *YB-1*$^{+/-}$ cells, in spite of the reduced content of YB-1 protein. We examined whether p21 levels were changed in these wild-type and mutant ES cells. Western blot analysis of heterozygously disrupted mutant cells (YB-1$^{+/-}$) also showed a reduction in YB-1 protein levels, but no change of p21 levels was observed in these wild and mutant ES cells (Fig. 4).

Discussion

To clarify the biological role of YB-1 by modulating the amount of cellular YB-1, cell lines defective in the *YB-1* gene should be useful. In the present study, we have generated *YB-1*$^{+/-}$ cell lines using a gene-targeting techniques. The cell lines established have a sequence alteration in a defined region of one allele of the *YB-1* gene, and display a significant depletion of YB-1 mRNA (approximately 50%). Consistent with the reduction in mRNA transcripts, the protein level of the *YB-1*$^{+/-}$ cells was reduced to approximately 50–60%, compared with that of *YB-1*$^{+/+}$ cells. In this study, insertion of the neomycin (*neo*) cassette resulted in deletion of a 1.8-kb region of the *YB-1* gene, containing a part of exon 5 and all of exon 6. The mutant allele may produce a truncated protein and this protein may function in a dominant-negative manner. We could not detect

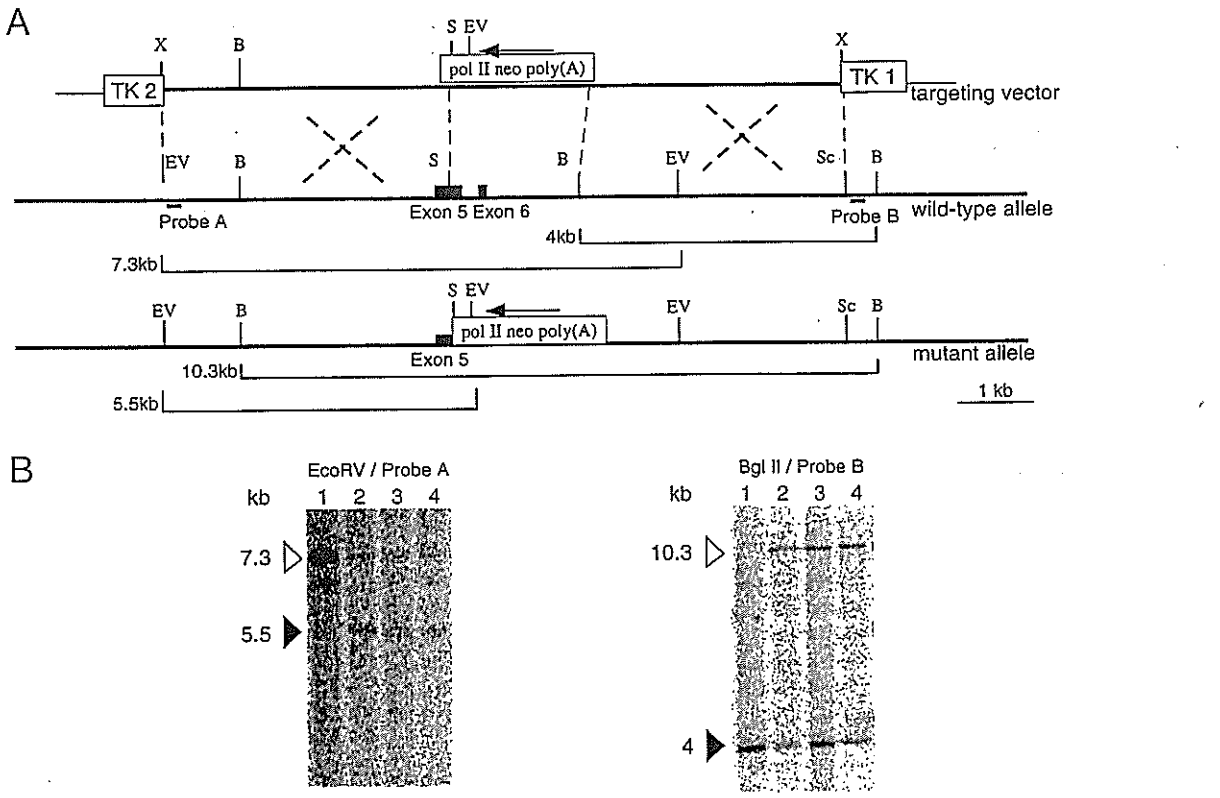

Fig. 1. Targeted disruption of the *mouse YB-1* gene. (A) Configurations of the intact and mutated alleles. The targeting vector carried approximately 8.4 kb of the genomic sequence, within which a part of exon 5 and all of exon 6 was replaced by the *pol*II-*neo*-poly(A) cassette. Restriction enzyme sites are shown; *Xho*I (X), *Bgl*II (B), *Sal*I (S), *Eco*RV (EV), and *Sac*I (Sc). Thick lines indicate the genomic sequence and thin lines represent the bacterial plasmid. The 5′ to 3′ orientation of the *mouse YB-1* gene is left to right, while the 5′ to 3′ orientation of the *pol*II *neo* pA cassette, HSV-1 thymidine kinase gene (TK1) and HSV-2 thymidine kinase gene (TK2) is right to left. Positions of the 5′- and 3′-probes, indicated as probes A and B, respectively, are also shown. (B and C) Southern blot analysis of the DNA isolated from the embryonic stem cell lines. An *Eco*RV digest hybridized with probe A (5′ internal), and a *Bgl*II digest hybridized with probe B (3′ flanking) yielded a wild-type band and a mutant band as indicated. In both cases, genotypes of cells are shown as follows: lane 1, *YB-1*$^{+/+}$; lane 2, clone 1 of *YB-1*$^{+/-}$; lane 3, clone 2 of *YB-1*$^{+/-}$; lane 4, clone 5 of *YB-1*$^{+/-}$.

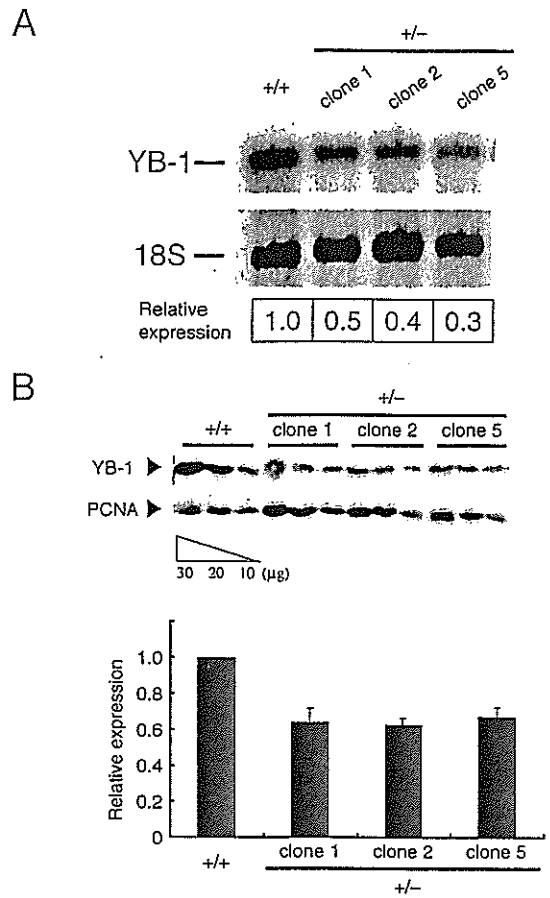

Fig. 2. (A) Northern blot analysis of the *YB-1* mRNA isolated from the germ-line-transmitted embryonic stem cell lines. Total RNA (10 μg) from each cell line was separated on a 1% agarose gel containing 2.2 *M* formaldehyde, transferred to a Hybond N+ membrane, and hybridized with ^{32}P-labeled YB-1 cDNA (1060 bp). Relative expression levels of *YB-1* mRNA are presented following normalization to 18S ribosome RNA. (B) Immunoblot analysis of the YB-1 protein isolated from the germ-line-transmitted embryonic stem cell lines. To detect the protein level of YB-1 semi-quantitatively, 30, 20, and 10 μg of total cell lysate were applied to adjacent lanes. The amount of YB-1 in each cell line was quantitated by immunoblot analysis of the same membrane with anti-PCNA antibody and is expressed relative to the amount of PCNA. Relative expression of YB-1 is presented following normalization to PCNA levels.

Table 1. Doubling time of YB-1$^{+/+}$ and YB-1$^{+/-}$ ES cells

Cell lines	Doubling time (h)
YB-1$^{+/+}$	10.2
YB-1$^{+/-}$	
Clone 1	10.0
Clone 2	9.0
Clone 5	10.2

Each value is the mean of duplicate determinations.

the NH_2-terminally truncated form of the YB-1 protein by immunoblotting using an antibody against the NH_2-terminus of YB-1 (data not shown). Although we tried to establish double knockout ES cells (*YB-1*$^{-/-}$) by subsequent culture of heterozygous mutant cells in an elevated concentration of G418, we could not isolate homozygous null mutant ES cells, suggesting that a complete lack of YB-1 may be lethal in ES cells. We have previously shown that YB-1 is directly involved in multidrug-resistance 1 gene activation at the transcriptional level.

Table 2. A. Sensitivity of YB-1$^{+/+}$ and YB-1$^{+/-}$ ES cells to various drugs on MTS assay

Agent	IC_{50}[1] for *YB-1*$^{+/+}$	Relative sensitivity[2] *YB-1*$^{+/-}$		
		Clone 1	Clone 2	Clone 5
Cisplatin (μ*M*)	20.0	0.5	0.3	0.2
Mitomycin C (μ*M*)	9.0	0.3	0.2	0.1
Etoposide (μ*M*)	0.6	1.5	0.5	0.2

B. Sensitivity of YB-1$^{+/+}$ and YB-1$^{+/-}$ ES cells to various drugs on colonogenic assay

Agent	C_{90}[1] for *YB-1*$^{+/+}$	Relative sensitivity[2] *YB-1*$^{+/-}$		
		Clone 1	Clone 2	Clone 5
Cisplatin (μ*M*)	1.5	0.6	0.7	0.4
Mitomycin C (μ*M*)	0.16	0.6	0.6	0.5
Etoposide (μ*M*)	0.07	1.2	1.2	0.9
UV (J/m^2)	3.8	1.1	0.9	0.9
γ-Rays (Gy)	5.4	1.0	1.2	0.8

1) The IC_{50} of *YB-1*$^{+/+}$ and *YB-1*$^{+/-}$ cells for each agent was determined by MTS assay and the IC_{90} was determined by colony formation assays.
2) The relative sensitivity of each clone of *YB-1*$^{+/-}$ ES cells was determined by dividing the IC_{50} or IC_{90} value for each cell line by that of *YB-1*$^{+/+}$ ES cell line. Values are means derived from two separate experiments.

YB-1 is directly required for basal promoter activation in response to genotoxic stresses, including carcinogens, anticancer agents, and UV irradiation.[7–9] Also, varying levels of expression of the YB-1 protein are associated with many biological phenomena, including cell proliferation and transformation.[5,21,22,28,29] Determining how YB-1 plays a role in biological processes in eukaryotic cells is therefore important. We have shown that YB-1 is located mainly in the cytoplasm, and then accumulates in the nucleus when cells are exposed to genotoxic stress.[16] We have observed that YB-1 is overexpressed in human cancer cells lines that are resistant to cisplatin, and that the amount of YB-1 correlates with the sensitivity of these cells to anti-cancer drugs, cisplatin, mitomycin C and UV irradiation.[15] However, the previously observed inverse correlation between YB-1 levels and drug sensitivity in human cancer cell lines may result from genetic and epigenetic differences unrelated to YB-1 among these cell lines. Single knockout ES cells of various genes, such as O^6-methylguanine-DNA methyltransferase (MGMT) and multiple drug related protein 1 (MRP1), which are associated with DNA repair and drug resistance, respectively, displayed a higher sensitivity to anticancer drugs as compared with their wild-type counterparts.[30,31] In principle, these particular ES cell lines, having a defect in one allele of the *YB-1* gene, could facilitate studies on the biological role of the YB-1 protein.

Cisplatin is widely used in treating a variety of human malignancies. Resistance to this agent is mediated through pleiotropic mechanisms, including decreased drug accumulation, detoxification of the drug, and DNA repair.[32,33] We have also shown that YB-1 levels correlate with sensitivity to cisplatin, suggesting that YB-1 is directly involved in both the cellular response to cisplatin and cisplatin resistance.[15] We therefore examined the sensitivity of the *YB-1*$^{+/-}$ cells to various anticancer drugs, X-rays, and UV irradiation. YB-1$^{+/-}$ cells showed an increased sensitivity to cisplatin and mitomycin C; drugs which induce cross-linking of DNA. Conversely, no dramatic difference in sensitivity to etoposide compared to *YB-1*$^{+/+}$ cells was noted in the MTS assay, or the colony formation assay. Essentially, these results are consistent with the sensitivity levels of YB-1 antisense transfectants, in terms of colony formation.[15]

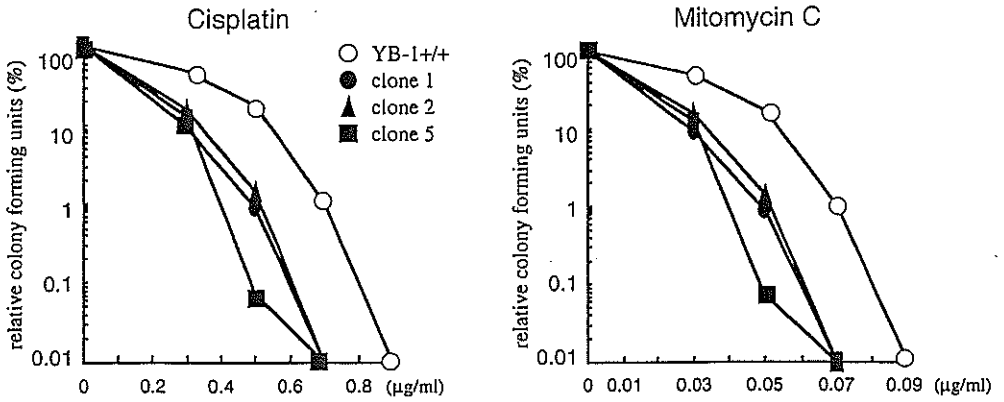

Fig. 3. Dose-response curve to anticancer drugs of *YB-1*$^{+/+}$ and *YB-1*$^{+/-}$ ES cells. Approximately 500 cells were plated on gelatin-coated 6-well plates and incubated in the absence of any drug for 24 h. The cells were then exposed to various concentrations of drugs for 7 days, and the remaining number of colonies was counted; 100% corresponds to the colony number of the same cell line in the absence of any drug. Data points: average values for triplicate dishes.

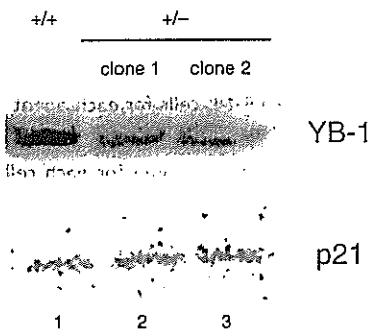

Fig. 4. Immunoblot analysis of the YB-1 and p21 proteins isolated from the germ-line-transmitted embryonic stem cell lines. Total cell lysate (20 μg) was applied to adjacent lanes. In both cases, genotypes of cells are shown as follows: lane 1, *YB-1*$^{+/+}$ ES; lane 2, clone 1 of *YB-1*$^{+/-}$ ES; lane 3, clone 2 of *YB-1*$^{+/-}$ ES.

We consider that the MTS assay can be markedly affected by the rate of cell death, rather than clonogenic survival, and that in turn, can be dependent on the proportion of cells undergoing apoptosis. This may be the reason why we still observed a sensitivity to etoposide in the MTS assay of *YB-1*$^{+/-}$ cells. ES cells with the *YB-1*$^{+/-}$ background had a 60% expression level of YB-1 protein compared to *YB-1*$^{+/+}$ cells. This reduced protein level in *YB-1*$^{+/-}$ cells clearly reflects the sensitivity level of the heterozygous mutant cells, as expected from the findings that stoichiometric amounts of YB-1 protein are needed for sensitivity to cisplatin and mytomicin C. These results indicate that YB-1 is involved in the cellular response to DNA-damaging agents, especially DNA-cross-linking agents. However, in this study no apparent difference in sensitivity to UV irradiation was found between *YB-1*$^{+/-}$ and *YB-1*$^{+/+}$ cells, as compared with the previous study.[15] The IC_{50} dose for UV irradiation of wild-type ES cell was 3.8 (J/m^2), compared to 7.0 (J/m^2) in KB cells. This finding may be a result of the genetic and epigenetic differences between human cancer cell lines and ES cells.

YB-1 has been shown to bind preferentially to cisplatin-modified DNA, apurinic DNA, and RNA containing 8-oxoguanine,[18,19,26] suggesting that this protein may bind preferentially to structurally altered DNA.[17] Several nuclear proteins that recognize cisplatin-DNA adducts have been characterized.[32,34] Among the HMG protein family, HMG1 and HMG2 have been shown to bind specifically to DNA that contains cisplatin-induced intrastrand cross-links[35] and to sensitize cancer cells to cisplatin.[36,37] Also, IXRI, a yeast protein containing an HMG box, confers sensitivity to cisplatin, though a correlation between the cellular levels of HMG proteins and the repair of damaged DNA has not been demonstrated.[38] It has been established that various repair processes, mainly nucleotide excision repair and mismatch repair, are involved in repair of the cisplatin-induced DNA damage.[39] Cells deficient in DNA repair have been found to be particularly sensitive to cisplatin. Mammalian cells defective in XPF- and ERCC-1, among the proteins involved in nucleotide excision repair, are extremely sensitive to cisplatin.[40] In fact, DNA repair activity has been implicated as a main cause of the resistance of many cell lines to cisplatin. Thus, the cellular sensitivity to cisplatin may be determined by a dynamic interaction between DNA damage recognition processes and DNA repair proteins. We have demonstrated that YB-1 interacts directly with proliferating cell nuclear antigen and p53, which are essential proteins in DNA replication and repair.[18,20] We have also shown that overexpression of the p53-associated protein p73, involved in DNA repair and apoptosis, increases cellular levels of YB-1,[41] and that YB-1 possesses 3′-5′ DNA exonuclease activity. YB-1 may recognize DNA damaged by a DNA-cross-linking agent, such as cisplatin, and be involved in the process of DNA repair, possibly through interaction with other repair-related proteins.

Recent studies using heterozygous DT40 YB1b (+/−) cells with one copy of the wild-type Chk-YB-1b allele showed a slower rate of growth, abnormal cell morphology, increased cell size, and increased genomic DNA content, compared to wild-type DT40 cells, and it was concluded that YB-1 plays an important role in cell proliferation.[27] In contrast, we found no such apparent growth retardation or abnormal cell morphology of *YB-1*$^{+/-}$ ES cells compared with the wild type. We also found no difference of p21 levels between the two (Fig. 4). This may be due to the following reasons: 1) The level of YB-1 protein in *YB-1*$^{+/-}$ cells was approximately 60% of that of *YB-1*$^{+/+}$ cells and this level of YB-1 protein may be sufficient for the proliferation of *YB-1*$^{+/-}$ cells. 2) DT40 cells were derived from chicken B lymphocytes and do not express p53. Therefore, mouse ES cells may differ greatly from DT40 cells with respect to genetic background, especially regarding the cell cycle and apoptosis control processes. Additional studies are required to determine the differences in phenotype between mouse ES and chicken DT40 cells. Also, the cellular level of YB-1 is associated with tumor growth in ovarian cancers, lung cancers, and breast cancers.[21–23] At present, we have not been able to establish a homozygous null mutant in ES cells. Taken together, these findings suggest that the YB-1 function may be essential for cell viability and proliferation.

In conclusion, we have established YB-1 single knockout cell lines, using gene targeting techniques, and shown that the extent of YB-1 expression correlates with cellular sensitivity to the cytotoxic effects of cisplatin and mitomycin C. YB-1 appears to protect cells or DNA integrity from the toxic insults associated with exposure to DNA-damaging agents. YB-1 is therefore expected to be involved in variety of biological roles, including transcription, cell proliferation, drug resistance, and

DNA repair. To elucidate these physiological roles of the YB-1 protein, establishment of mouse lines defective in *YB-1* genes is in progress. For more definitive studies, designed to evaluate the precise role of the YB-1 protein *in vivo*, the generation of conditional YB-1 mutants may be necessary.

This work was supported by grants from the Ministry of Education, Culture, Sports, Science and Technology of Japan, from the Ministry of Health, Labour and Welfare of Japan, and from Kyushu University Interdisciplinary Programs in Education and Projects in Research Development.

1. Wolffe AP, Tafuri S, Ranjan M, Familari M. The Y-box factors: a family of nucleic acid binding proteins conserved from *Escherichia coli* to man. *New Biol* 1992; 4: 290–8.
2. Makino Y, Ohga T, Toh S, Koike K, Okumura K, Wada M, Kuwano M, Kohno K. Structural and functional analysis of the human Y-box binding protein (YB-1) gene promoter. *Nucleic Acids Res* 1996; 24: 1873–8.
3. Toh S, Nakamura T, Ohga T, Koike K, Uchiumi T, Wada M, Kuwano M, Kohno K. Genomic organization of the human Y-box protein (YB-1) gene. *Gene* 1998; 206: 93–7.
4. Didier DK, Schiffenbauer J, Woulfe SL, Zacheis M, Schwartz BD. Characterization of the cDNA encoding a protein binding to the major histocompatibility complex class II Y box. *Proc Natl Acad Sci USA* 1988; 85: 7322–6.
5. Ladomery M, Sommerville J. A role for Y-box proteins in cell proliferation. *BioEssays* 1995; 17: 9–11.
6. Wolffe AP. Structural and functional properties of the evolutionarily ancient Y-box family of nucleic acid binding proteins. *BioEssays* 1994; 16: 245–51.
7. Uchiumi T, Kohno K, Tanimura H, Matsuo K, Sato S, Uchida Y, Kuwano M. Enhanced expression of the human multidrug resistance 1 gene in response to UV light irradiation. *Cell Growth Differ* 1993; 4: 147–57.
8. Asakuno K, Kohno K, Uchiumi T, Kubo T, Sato S, Isono M, Kuwano M. Involvement of a DNA binding protein, MDR-NF1/YB-1, in human MDR1 gene expression by actinomycin D. *Biochem Biophys Res Commun* 1994; 199: 1428–35.
9. Ohga T, Uchiumi T, Makino Y, Koike K, Wada M, Kuwano M, Kohno K. Direct involvement of the Y-box binding protein YB-1 in genotoxic stress-induced activation of the human multidrug resistance 1 gene. *J Biol Chem* 1998; 273: 5997–6000.
10. Furukawa M, Uchiumi T, Nomoto M, Takano H, Morimoto RI, Naito S, Kuwano M, Kohno K. *J Biol Chem* 1998; 273: 10550–5.
11. Swamynathan SK, Nambiar A, Guntaka RV. Role of single-stranded DNA regions and Y-box proteins in transcriptional regulation of viral and cellular genes. *FASEB J* 1998; 2: 515–22.
12. Matsumoto K, Wolffe AP. Gene regulation by Y-box proteins: coupling control of transcription and translation. *Trends Cell Biol* 1998; 8: 318–23.
13. Sommerville J. Activities of cold-shock domain proteins in translation control. *BioEssays* 1999; 21: 319–25.
14. Tafuri SR, Familari M, Wolffe AP. A mouse Y box protein, MSY1, is associated with paternal mRNA in spermatocytes. *J Biol Chem* 1993; 268: 12213–20.
15. Ohga T, Koike K, No M, Makino Y, Itagaki Y, Tanimoto M, Kuwano M, Kohno, K. Role of the human Y box-binding protein YB-1 in cellular sensitivity to the DNA-damaging agents cisplatin, mitomycin C, and ultraviolet light. *Cancer Res* 1996; 56: 4224–8.
16. Koike K, Uchiumi T, Ohga T, Toh S, Wada M, Kohno K, Kuwano M. Nuclear translocation of the Y-box binding protein by ultraviolet irradiation. *FEBS Lett* 1997; 417: 390–4.
17. Hasegawa SL, Doetsch PW, Hamilton KK, Martin AM, Okenquist SA, Lenz J, Boss JM. DNA binding properties of YB-1 and dbpA: binding to double-stranded, single-stranded, and abasic site containing DNAs. *Nucleic Acids Res* 1991; 19: 4915–20.
18. Ise T, Nagatani G, Imamura T, Kato K, Takano H, Nomoto M, Izumi H, Ohmori H, Okamoto T, Ohga T, Uchiumi T, Kuwano M, Kohno K. Transcription factor Y-box binding protein 1 binds preferentially to cisplatin-modified DNA and interacts with proliferating cell nuclear antigen. *Cancer Res* 1999; 59: 342–6.
19. Hayakawa H, Uchiumi T, Fukuda T, Ashizuka M, Kohno K, Kuwano M, Sekiguchi M. Binding capacity of human YB-1 protein for RNA containing 8-oxoguanine. *Biochemistry* 2002; 41: 12739–44.
20. Okamoto T, Izumi H, Imamura T, Takano H, Ise T, Uchiumi T, Kuwano M, Kohno K. Direct interaction of p53 with the Y-box binding protein, YB-1: a mechanism for regulation of human gene expression. *Oncogene* 2000; 19: 6194–202.
21. Kamura T, Yahata H, Amada S, Ogawa S, Sonoda T, Kobayashi H, Mitsumoto M, Kohno K, Kuwano M, Nakano H. Is nuclear expression of Y box-binding protein-1 a new prognostic factor in ovarian serous adenocarcinoma? *Cancer* 1999; 85: 2450–4.
22. Shibahara K, Sugio K, Osaki T, Uchiumi T, Maehara Y, Kohno K, Yasumoto K, Sugimachi K, Kuwano M. Nuclear expression of the Y-box binding protein, YB-1, as a novel marker of disease progression in non-small cell lung cancer. *Clin Cancer Res* 2001; 7: 3151–5.
23. Janz M, Harbeck N, Dettmar P, Berger U, Schmidt A, Jurchott K, Schmitt M, Royer HD. Y-box factor YB-1 predicts drug resistance and patient outcome in breast cancer independent of clinically relevant tumor biologic factors HER2, uPA and PAI-1. *Int J Cancer* 2001; 97: 278–82.
24. Mansour SL, Thomas KR, Capecchi MR. Disruption of the proto-oncogene int-2 in mouse embryo-derived stem cells: a general strategy for targeting mutations to non-selectable genes. *Nature* 1988; 336: 348–52.
25. Tsuzuki T, Fujii Y, Sakumi K, Tominaga Y, Nakao K, Sekiguchi M, Matsushiro A, Yoshimura Y, Morita T. Targeted disruption of the Rad51 gene leads to lethality in embryonic mice. *Proc Natl Acad Sci USA* 1996; 93: 6236–40.
26. Izumi H, Imamura T, Nagatani G, Ise T, Murakami T, Uramoto H, Torigoe T, Ishiguchi H, Yoshida Y, Nomoto M, Okamoto T, Uchiumi T, Kuwano M, Funa K, Kohno K. Y box-binding protein-1 binds preferentially to single-stranded nucleic acids and exhibits 3′→5′ exonuclease activity. *Nucleic Acids Res* 2001; 29: 1200–7.
27. Swamynathan S, Varma B, Weber K, Guntaka R. Targeted disruption of one allele of the Y-box protein gene, Chk-YB-1b, in DT40 cells results in major defects in cell cycle. *Biochem Biophys Res Commun* 2002; 296: 451–7.
28. Oda Y, Sakamoto A, Shinohara N, Ohga T, Uchiumi T, Kohno K, Tsuneyoshi M, Kuwano M, Iwamoto Y. Nuclear expression of YB-1 protein correlates with P-glycoprotein expression in human osteosarcoma. *Clin Cancer Res* 1998; 4: 2273–7.
29. Shibao K, Takano H, Nakayama Y, Okazaki K, Nagata N, Izumi H, Uchiumi T, Kuwano M, Kohno K, Itoh H. Enhanced coexpression of YB-1 and DNA topoisomerase II alpha genes in human colorectal carcinomas. *Int J Cancer* 1999; 83: 732–7.
30. Lorico A, Rappa G, Flavell RA, Sartorelli AC. Double knockout of the MRP gene leads to increased drug sensitivity *in vitro*. *Cancer Res* 1996; 56: 5351–5.
31. Tominaga Y, Tsuzuki T, Shiraishi A, Kawate H, Sekiguchi M. Alkylation-induced apoptosis of embryonic stem cells in which the gene for DNA-repair, methyltransferase, had been disrupted by gene targeting. *Carcinogenesis* 1997; 18: 889–96.
32. Chu G. Cellular responses to cisplatin. The roles of DNA-binding proteins and DNA repair. *J Biol Chem* 1994; 269: 787–90.
33. Stavrovskaya A. A cellular mechanisms of multidrug resistance of tumor cells. *Biochemistry (Mosc)* 2000; 65: 95–106.
34. Zamble DB, Lippard SJ. Cisplatin and DNA repair in cancer chemotherapy. *Trends Biochem Sci* 1995; 20: 435–9.
35. Timmer-Bosscha H, Mulder NH, de Vries EG. Modulation of *cis*-diamminedichloroplatinum(II) resistance: a review. *Br J Cancer* 1992; 66: 227–38.
36. Arioka H, Nishio K, Ishida T, Fukumoto H, Fukuoka K, Nomoto T, Kurokawa H, Yokote H, Abe S, Saijo N. Enhancement of cisplatin sensitivity in high mobility group 2 cDNA-transfected human lung cancer cells. *Jpn J Cancer Res* 1999; 90: 108–15.
37. He Q, Liang CH, Lippard SJ. Steroid hormones induce HMG1 overexpression and sensitize breast cancer cells to cisplatin and carboplatin. *Proc Natl Acad Sci USA* 2000; 97: 5768–72.
38. Brown SJ, Kellett PJ, Lippard SJ. Ixr1, a yeast protein that binds to platinated DNA and confers sensitivity to cisplatin. *Science* 1993; 261: 603–5.
39. Damia G, Imperatori L, Stefanini M, D'Incalci M. Sensitivity of CHO mutant cell lines with specific defects in nucleotide excision repair to different anti-cancer agents. *Int J Cancer* 1996; 66: 779–83.
40. De Silva IU, McHugh PJ, Clingen PH, Hartley JA. Defects in interstrand cross-link uncoupling do not account for the extreme sensitivity of ERCC1 and XPF cells to cisplatin. *Nucleic Acids Res* 2002; 30: 3848–56.
41. Uramoto H, Izumi H, Ise T, Tada M, Uchiumi T, Kuwano M, Yasumoto K, Funa K, Kohno K. p73 interacts with c-Myc to regulate Y-box-binding protein-1 expression. *J Biol Chem* 2002; 277: 31694–72.

Interleukin-1β Represses *MRP2* Gene Expression Through Inactivation of Interferon Regulatory Factor 3 in HepG2 Cells

Keiji Hisaeda,[1] Akihiko Inokuchi,[1] Takanori Nakamura,[1] Yukihide Iwamoto,[2] Kimitoshi Kohno,[3] Michihiko Kuwano,[4] and Takeshi Uchiumi[1]*

The human multidrug resistance protein 2 (*MRP2*/ABCC2), expressed on the bile canalicular membrane, mediates the multispecific efflux of several organic anions, including conjugates of glucuronate, sulfate, and glutathione. Expression of MRP2 can be altered in response to environmental stimuli such as cholestasis and jaundice. We previously reported that *MRP2* mRNA expression levels are decreased in the nontumorous part of hepatitis C virus-infected human liver tissues, and that inflammatory cytokines inhibit *MRP2* expression in human hepatic (HepG2) cells. We investigated the molecular mechanisms by which inflammatory cytokines modulate *MRP2* gene expression in hepatic cells. Treatment of human hepatic cells with interleukin-1β (IL-1β) or tumor necrosis factor α resulted in a decrease in the protein and mRNA levels of *MRP2*. IL-1β inhibited the transcriptional activity of *MRP2* promoter constructs by 40%, and this inhibition of *MRP2* promoter activity was mediated through the interferon stimulatory response element (ISRE). Electrophoretic mobility shift assays with IL-1β-treated nuclear extracts showed a decrease in the formation of DNA protein complexes, specifically those including interferon regulatory factor 3 (IRF3). Expression of recombinant human IRF3 increased *MRP2* promoter activity. Treatment with a specific extracellular signal-regulated kinase inhibitor relieved IL-1β-induced *MRP2* mRNA downregulation and abrogated the binding of IRF3 to the ISRE element. In conclusion, IL-1β induces downregulation of the *MRP2* gene by inactivating IRF3 binding to ISRE on the *MRP2* promoter in human hepatic cells; this inactivation is accomplished via interference with the extracellular signal-regulated kinase pathway. (HEPATOLOGY 2004;39:1574–1582.)

Transport proteins in the basolateral and canalicular membranes of hepatocytes mediate transport of organic solutes into and from the liver. Biliary elimination of both endogenous compounds and exogenous drugs or poisons is a major physiological self-defense role of various transporters.[1] One of the major transport systems of this type involves the adenosine triphosphate binding cassette (ABC) transporter family. Among the numerous ABC transporters, P-glycoprotein (P-gp/ABCB1) and multidrug resistance protein 2 (*MRP2*/ABCC2) have been shown to mediate transport of cationic and anionic compounds into bile, and bile salt exporting pump (BSEP/ABCB11) has been shown to export bile acids.[2,3] *MRP2* initially was identified as a multispecific organic anion transporter in the canalicular membrane of hepatocytes and was shown to transport a wide range of conjugated compounds, including leukotriene C4, glucuronidase and sulfated molecules, and molecules conjugated to glutathione.[4–6] Inherited defects in *MRP2* result in Dubin-Johnson syndrome, a congenital disease associated with chronic hyperbilirubinemia and

Abbreviations: ABC transporter, adenosine triphosphate binding cassette transporter; P-gp, P-glycoprotein; MRP2, multidrug resistance protein 2; IL, interleukin; IRF3, interferon regulatory factor 3; RANTES, regulated on activation, normal T cell expressed and secreted; HCV, hepatitis C virus; TNFα, tumor necrosis factor α; ERK, extracellular signal-regulated kinase; ISRE, interferon stimulatory response element; PCR, polymerase chain reaction; C/EBP, CCAAT enhancer-binding protein; HNF, hepatocyte nuclear factor; USF, upstream stimulatory factor; EMSA, electrophoretic mobility shift assay; NE, nuclear extract; RXR, retinoid X receptor.

From the Departments of [1]Medical Biochemistry and [2]Orthopedic Surgery, Graduate School of Medical Sciences, Kyushu University, Fukuoka, Japan; the [3]Department of Molecular Biology, University of Occupation and Environmental Health, Fukuoka, Japan; and the [4]Research Center for Innovative Cancer Therapy of the 21st Century COE Program for Medical Science, Kurume University, Fukuoka, Japan.

Received September 30, 2003; accepted February 13, 2004.

Supported by the Second-Term Comprehensive Ten-Year Strategy for Cancer Control from the Ministry of Health and Welfare of Japan and by the Cancer Research Fund from the Ministry of Education, Culture, Sports, Science, and Technology.

Address reprint requests to: Takeshi Uchiumi, MD, PhD, Department of Medical Biochemistry, Graduate School of Medical Sciences, Kyushu University, 3-1-1 Maidashi, Fukuoka 812-8582, Japan. E-mail: uchiumi@biochem1.med.kyushu-u.ac.jp; fax: 81-92-642-6203.

Published online in Wiley InterScience (www.interscience.wiley.com).

DOI 10.1002/hep.20216

jaundice.[7–9] Liver diseases are characterized by disturbances in the hepatobiliary transport of endogenous and exogenous compounds. Hepatic expression of ABC transporters can be influenced by a number of endogenous and environmental factors. Inflammation is induced under various pathological conditions, such as carcinogenesis, cholestasis, and regeneration by partial hepatectomy and by lipopolysaccharides.[10–14] Administrations of inflammatory cytokines interleukin (IL)-6 and IL-1β has been shown to result in a 20% to 60% decrease in the mRNA levels of *MRP2*, organic anion-transporting polypeptide 1, organic anion-transporting polypeptide 2, and bile salt exporting pump in the mouse liver compared with untreated controls.[15] The decreased hepatic expression of these transporters affects the cellular efflux of various physiological compounds, suggesting that these cytokines may play a key role in the hepatic expression of anion transporters in inflammatory cholestasis.[15] Altered expression of the organic anion-transporting polypeptide and Mrp transporters also is expected to influence the pharmacokinetics of various drugs that are transported by these proteins.

The transcription factor interferon regulatory factor 3 (IRF3) is expressed constitutively in many cell types, and its expression is thought to contribute to self-defense from viral infection by inducing type I interferons.[16,17] IRF3 is required for the expression of interferon β and the chemokine regulated on activation, normal T cell expressed and secreted (RANTES) in response to viral infection. In unstimulated cells, IRF3 is present dominantly in the cytoplasm and is phosphorylated in the N terminal domain. After viral infection, the C terminal domain of IRF3 is phosphorylated, leading to dimerization and interaction with the coactivator CBP/p300.[18] This complex is then translocated to the nucleus, where it activates a promoter containing the IRF3 binding site.

We previously compared the expression of ABC transporters between the hepatitis C virus (HCV)-infected and non-HCV-infected liver in patients with hepatic cancers and reported that the expression levels of *MRP2* mRNA and MRP2 protein were decreased significantly and specifically in the nontumorous part of HCV-infected liver tissue.[19] However, the expression levels of other ABC transporters—*MDR1*, *MDR3*, *MRP1*, and *MRP3*—were not significantly different between the HCV-infected and non-HCV-infected liver.[19] We hypothesized that the downregulation of *MRP2* mRNA levels after cytokine treatment occurred primarily at the transcriptional level, and that this reduction in *MRP2* transcription could be the result of alteration in regulatory nuclear transcription factors. We previously characterized regulatory elements in the human *MRP2* promoter in liver cells.[20] In the present study, we show that *MRP2* mRNA transcription decreased 24 hours after IL-1β and tumor necrosis factor α (TNFα) treatment. Nuclear extract treated with IL-1β showed a marked decrease in DNA protein complexes, including IRF3 complexes, and nuclear accumulation of IRF3 was decreased by treatment with IL-1β. The IL-1β–induced *MRP2* mRNA downregulation was relieved by a specific extracellular signal-regulated kinase (ERK) inhibitor. We hypothesize that this inflammatory cytokine-induced downregulation of MRP2 is the result of reductions in both the nuclear accumulation of IRF3 and the binding of IRF3 to interferon stimulatory response element (ISRE), and that these reductions occur via the ERK pathway.

Materials and Methods

Cell Culture. Human hepatoblastoma HepG2 cells were cultured in Dulbecco's modified Eagle's medium (Nissui Seiyaku, Tokyo, Japan) containing 10% fetal calf serum.[19,20] Normal human hepatocytes hNHeps (Sanko Junyaku, Japan) were cultured according to the manufacture's protocol.

Antibodies and Drugs. The antibodies used in these experiments are as follows: MRP2 (M2III-6; Alexis, San Diego, CA), P-gp (C219; Centacor, Malvern, PA), IRF3 (FL425; Santa Cruz Biotech, Santa Cruz, CA), high mobility group protein-I (T-16; Santa Cruz Biotech), and glucose-6-phosphate dehydrogenase (A9521; Sigma-Aldrich, Saint Louis, MO). All IRFs and Sp1 antibodies were purchased from Santa Cruz Biotech. The drugs Actinomycin D, PD98059, SB203580, and SP600125 were purchased from Carbiochem (San Diego, CA).

Preparation of Protein. For whole-cell lysate, cells were washed with ice cold phosphate-buffered saline and solubilized in 0.5 mL of radio-immunoprecipitation assay buffer (50 mM Tris HCl, 150 mM NaCl, 1% Triton X-100, 0.1% SDS, 0.5% deoxycholate, 1 mM phenylmethyl sulfonyl fluoride, and 1 mg/mL trypsin inhibitor) for 30 minutes on ice, then centrifuged at 15,000*g* for 10 minutes at 4°C. For nuclear and cytoplasmic extract, HepG2 and hNHeps were harvested by exposure to trypsin, resuspended in 200 μL of an ice-cold solution containing 10 mM HEPES NaOH (pH 7.9), 10 mM KCl, 0.2 mM ethylenediaminetetraacetic acid (EDTA), 0.2 mM ethylene glycol bis(βaminoethyl ether) (EGTA), 0.5 mM dithiothreitol, and 0.5 mM phenylmethylsulfonyl fluoride, and incubated on ice for 15 minutes. The cells were then lysed by passing 10 times through a 25-gauge needle attached to a 1-mL syringe, and the lysate was centrifuged for 40 seconds in a microcentrifuge. The supernatant was stored for cytoplasmic extract. The nuclear

pellet was resuspended in 100 μL of an ice-cold solution containing 20 mM HEPES NaOH (pH 7.9), 0.4 M NaCl, 0.75 mM spermidine, 0.15 mM spermine, 0.2 mM EDTA, 0.2 mM EGTA, 0.5 mM dithiothreitol, 0.5 mM phenylmethylsulfonyl fluoride, and 25% (vol/vol) glycerol, incubated for 30 minutes on ice with frequent gentle mixing, and then centrifuged for 20 minutes at 4°C in a microcentrifuge to remove insoluble material. The resulting supernatant (nuclear extract) was stored at −80°C.

Northern Blot Analysis. Total RNA was isolated using RNeasy spin columns (Qiagen, Hilden, Germany). 10 μg of total RNA from HepG2 cells was separated on a 1% formaldehyde-agarose gel and transferred to a membrane as described previously.[19] An *MRP2* complementary DNA (cDNA) probe (−28 to 513) was synthesized by polymerase chain reaction (PCR).

Reporter Gene Vector Constructs. The fragments of the 5′ region of the *MRP2* gene were ligated into the SacI and HindIII sites of pGL3-basic (Promega, Madison, WI). All plasmids were analyzed by restriction enzyme digestion, and the promoter inserts were sequenced. Site-directed mutagenesis of ISRE in p-491 MRP2 Luci was performed by a PCR-based method. The promoter sequence was amplified with Taq polymerase, a 5′-primer 491TAGGAGCTCTAGCGACTGATGCCAC and a 3′-primer that introduces a specific mutation into the ISRE region (5′-AGAAGCGAAACT-3′ to 5′-AcgtGCGcgtCT-3′). Amplification was also performed with a 5′-primer that introduces second specific mutation into the ISRE region and a 3′-primer AAGCTTGATTCCTGGACTGCGTC. Mutant constructs of CCAAT enhancer-binding protein β (C/EBPβ), hepatocyte nuclear factor 1 (HNF1), and upstream stimulatory factor (USF) were made using the same method (for C/EBPβ: 5′primer GAACTTTTAACCGCCTGTATTATG; 3′ primer AAGCTTGATTCCTGGACTGCGTC; for HNF1: 5′ primer GGCAAGGTCGGCGATTAAATGG; 3′ primer CCATTTAATCGCCGACCTTGCC; and for USF 5′ primer GGCTTTTTAGTTGTATGTCCATCC; 3′primer GGATGGACATTGTACTAAAAAGCC). A second PCR was then performed with Taq polymerase using the first PCR products as a template. The PCR product was cloned into pGEM-Teasy vector, which was subsequently digested with SacI and HindIII fragments. The fragments were ligated into the SacI and HindIII sites of pGL3-basic (Promega).

Luciferase Assay. HepG2 cells were transfected by the Lipofectamine method as previously described.[21] Briefly, a mixture of 5 μg of Lipofectamine 2000 (Life Technologies, Grand Island, NY), and 1 μg of reporter plasmid was incubated with the cells for 6 hours. Then, fresh medium containing 20 ng/mL IL-1β was added, and the cells were cultured for an additional 24 hours. In separate experiments, 20 μM PD98059 was administered for 30 minutes before IL-1β stimulation. 100 ng of pRL-TK (Promega) was cotransfected as a control for transfection. Luciferase activity was measured using a dual luciferase assay system (Promega). Twenty, 100, or 200 ng of Flag-only vector or Flag-IRF3 vector was cotransfected to investigate the effect of IRF3 function on the MRP2 promoter. Promoter activities are given as the mean ± SD of triplicate transfections. The level of significance of promoter activities in the presence of regular substrates was determined using Student's *t* test.

Electrophoretic Mobility Shift Assay (EMSA). Nuclear extracts were incubated for 30 minutes on ice in a final volume of 20 μL of reaction mixture containing 25 mM HEPES (pH 7.5), 100 mM KCl, 1 mM EDTA, 10% glycerol, 0.7 mM DTT, 10 ng of poly (dIdC), and 1 × 104 cpm of ^{32}P-labeled oligonucleotide probe in the absence or presence of wild-type or mutant (mt) competitors. The samples were electrophoresed on an 8% polyacrylamide gel (polyacrylamide/bisacrylamide ratio, 80:1) in Tris borate buffer. The DNA sequence of the sense strand of the wild-type MRP2ISRE oligonucleotide is GCAGCAGAAGCGAAACTGCAC, and that of the mutant MRP2ISRE is GCAGCAcgtGCGcgtCTGCAC. For supershift experiments, 2 μg of each antibody was added to the reaction mixture.

Results

IL-1β and TNFα Reduced the Expression of the MRP2 Protein and mRNA. We examined whether the MRP2 protein levels were affected by treatment of IL-1β and TNFα in HepG2 cells. Treatment with various doses of IL-1β and TNFα up to 20 ng/mL for 24 hours markedly reduced the MRP2 protein level in a dose-dependent manner, although P-gp levels remained the same. (Fig. 1A). We next examined the effect of IL-1β and TNFα stimulation on *MRP2* mRNA expression levels. *MRP2* mRNA levels were markedly reduced in a dose- and time-dependent manner (Fig. 1B,C). Treatment with IL-1β at 10 ng/mL or TNFα at 1 ng/mL for 24 hours reduced cellular *MRP2* mRNA levels to 40% or less of the levels in the untreated control (Fig. 1B). Treatment for 12 hours or longer with 20 ng/mL IL-1β or TNFα decreased *MRP2* mRNA levels to 30% to 40% of the levels in controls at time 0 (Fig. 1C). We next examined whether IL-1β signaling inhibitors could affect the IL-1β-induced downregulation of *MRP2* gene expression. IL-1β is known to regulate several signal transduction cascades, including the three main kinase cascades, mitogen-acti-

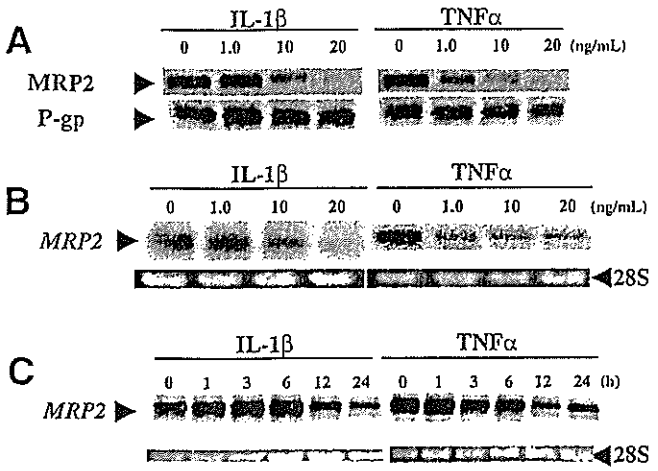

Fig. 1. Alteration of multidrug resistance protein 2 (MRP2) and P-glycoprotein (P-gp)/MDR1 protein and mRNA levels in HepG2 in response to interleukin-1β (IL-1β) or tumor necrosis factor-α (TNFα) administration. (A) For Western blot analysis, 200 μg of protein was loaded, and blots were incubated with an antibody, M2III-6 for MRP2 and C219 for P-gp/MDR1. (B,C) Northern blot analysis. (B) HepG2 cells were treated with the indicated dose of IL-1β (**left**) or TNFα (**right**) for 24 hours. (C) HepG2 cells were treated with 20 ng/mL IL-1β (**left**) or TNFα (**right**) for the indicated time. Ten micrograms total RNA was loaded and hybridized with *MRP2* cDNA. The results were representative of three experiments.

vated protein kinase-ERK, c-Jun NH_2-terminal kinase (JNK), and p38 mitogen-activated protein kinase.[22,23] Coadministration of SB203580 (p38 mitogen-activated protein kinase inhibitor) and SP600125 (JNK inhibitor) with IL-1β had no effect on the IL-1β-mediated downregulation of *MRP2* mRNA levels (Fig. 2, lanes 2, 3, and 5), whereas PD98059 (ERK1/2 inhibitor) almost completely relieved the downregulatory effect of IL-1β (Fig. 2, lanes 2 and 4). There seemed to be no inhibitory effect

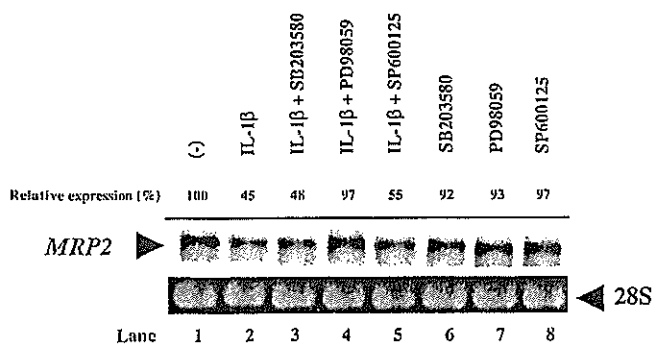

Fig. 2. Extracellular signal-regulated kinase (ERK) pathways were involved in interleukin-1β (IL-1β)-induced *MRP2* downregulation. 20 μM PD98059 (MEK1/2 inhibitor), 25 μM SB203580 (p38 inhibitor), or 20 μM SP600125 (JNK inhibitor) were pretreated for 30 minutes before IL-1β stimulation (20 ng/mL) in HepG2 cells. After 24 hours, total RNA were harvested and hybridized with multidrug resistance protein 2 (MRP2) cDNA. Relative *MRP2* mRNA expression levels are shown, compared with the expression in untreated cells. This result was representative of three experiments.

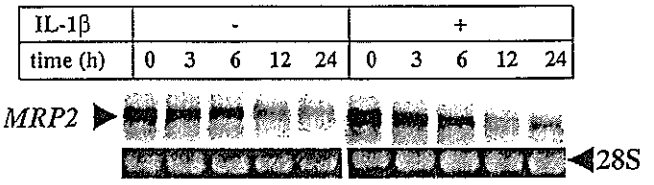

Fig. 3. Rates of *MRP2* mRNA decay. 5 μg/mL actinomycin D was incubated for 30 minutes with HepG2 cells, and interleukin-1β (IL-1β; 20 ng/mL) was administrated for the indicated time. Total RNA was harvested, and 10 μg of RNA was loaded on a 1% formaldehyde-agarose gel and transferred to a membrane. This result was representative of three experiments.

of PD98059 alone on *MRP2* mRNA expression (Fig. 2, lane 7). These results suggest that *MRP2* mRNA downregulation by IL-1β involves the ERK pathway.

To understand how *MRP2* mRNA expression was downregulated by IL-1β, we initially examined whether the stability of *MRP2* mRNA was altered. The *MRP2* mRNA stability was examined, in the absence or presence of IL-1β, by blocking synthesis with 5 μg/mL of actinomycin D (Fig. 3). We observed that *MRP2* mRNA was degraded at similar half-lives of approximately 12 hours under both conditions (Fig. 3), suggesting that IL-1β-induced downregulation of *MRP2* mRNA was not the result of destabilization of mRNA by IL-1β.

Human* MRP2 *Gene Promoter Activity was Inhibited by IL-1β Through an Interferon Stimulatory Response Element at −179/−146bp. We investigated human *MRP2* promoter activity in response to IL-1β administration using a series of 5′-promoter deletion analysis. Deleted promoter fragments were ligated into the reporter gene vector pGL3 basic and were transiently transfected into HepG2 cells. The luciferase activity of the complete series of 5′-deleted *MRP2* promoter constructs is shown in Fig. 4. Compared with p-1659, the luciferase activity decreased to 30% when p-491 was assayed, suggesting that a putative positive cis-element is localized in the −1659/−491 bp region. We also observed an approximately 50% increase in luciferase activity by p-179 as compared with p-491, suggesting that a negative regulatory element is localized in the −491/−179 bp region. Administration of IL-1β reduced *MRP2* promoter activity by 30% to 50% when p-2653, p-1659, p-491, and p-179 were assayed (Fig. 4). However, IL-1β failed to reduce the *MRP2* promoter activity when p-146 and p-21 constructs were assayed. These results suggested that a putative IL-1β response element is located on the −179/−146 region. We identified an ISRE within the −179/−146 region (Fig. 4). To examine whether mutations within the ISRE binding motif affected the downregulation of the *MRP2* promoter activity in response to IL-1β, we performed a mutagenesis analysis of the pro-

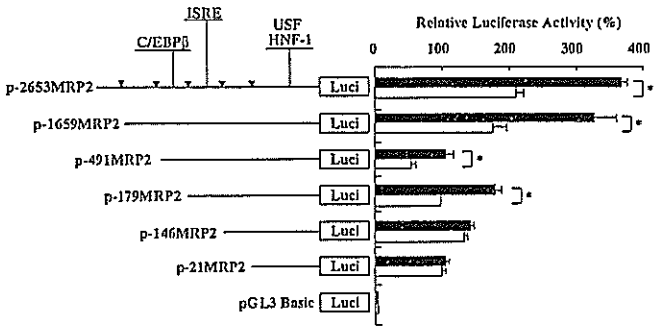

Fig. 4. Maps of the *MRP2* promoter luciferase constructs and the transcriptional activity of multidrug resistance protein 2 (MRP2) promoter-luciferase fusion plasmids transfected into HepG2 cells. Various lengths of human *MRP2* gene promoter plasmids containing the luciferase gene in the upstream region were constructed. Putative transcription factor binding sites on the *MRP2* promoter are also indicated. Luciferase activities were measured after 24 hours and were correlated for differences in transfection efficiency by *Renilla* luciferase activity, then normalized to the activity of the p-491 MRP2-Luci construct transfected into cells. Data are shown as the mean ± SD (error bars) of three independent experiments. $*P < .01$. ISRE, interferon stimulatory response element; USF, upstream stimulatory factor; HNF-1, hepatic nuclear factor 1.

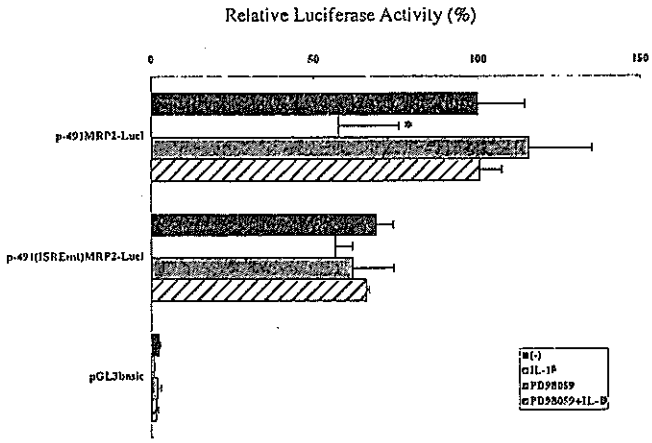

Fig. 6. Effects of PD98059 on interleukin-1β (IL-1β)-induced *MRP2* promoter suppression. p-491MRP2-Luci and p-491MRP2(ISREmt)-Luci were transfected into HepG2 cells. Six hours later, 20 μM PD98059 was administrated for 30 minutes and IL-1β was treated (20 ng/mL; 24 hours). This result was representative of three experiments. $*P < .05$. MRP2, multidrug resistance protein 2; ISRE, interferon stimulatory response element.

moter. The construct designed contained a specific mutation in the consensus sequence of ISRE on the *MRP2* promoter (AGAAGCGAAACT to AcgtGCGcgtCT). To check the adjacent transcription factors, we also made C/EBPβ, HNF 1, and USF mutant constructs (Fig. 5). We transfected the mutant p-491MRP2-Luci constructs into HepG2 cells in the absence or presence of IL-1β. Compared with the wild-type construct, the ISRE mutant reporter gene constructs showed a slightly lower basal activity in comparison with the wild type. Introduction of mutation into USF (USFmt) did not affect the basal promoter activity, whereas the HNFmt construct showed a marked decrease in the basal promoter activity, suggesting that HNF plays a key role in the *MRP2* basal promoter activity. C/EBPmt construct enhanced the basal promoter activity by approximately 170% compared with the wild-type construct, indicating a negative regulatory role of C/EBPβ. When the p-491 MRP2 ISREmt was treated with IL-1β, no suppression of reporter gene activity was observed. There was a significant decrease in the promoter activity of IL-1β-treated USFmt, HNFmt, and C/EBPβmt reporter constructs (Fig. 5). These results indicated that the ISRE element specifically contributes to both basal promoter activity and IL-1β responsive down-regulation in *MRP2* promoter constructs.

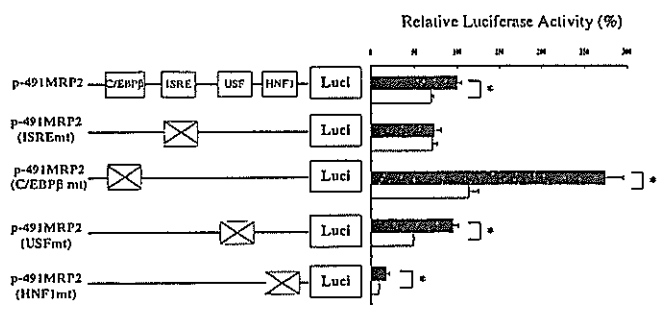

Fig. 5. Transcriptional activity of p-491 MRP2-Luci and 4 p-491 MRP2 mutant-Luci (interferon stimulatory response element [ISRE], C/EBPβ, hepatic nuclear factor 1 [HNF1], and upstream stimulatory factor [USF]) transfected into HepG2 cells with or without 20 ng/mL of interleukin-1β (IL-1β) for 24 hours. Various mutant forms of human *MRP2* gene promoter plasmids containing the luciferase gene in the upstream region were constructed. Luciferase activities were measured after 24 hours and were corrected for differences in transfection efficiency by *Renilla* luciferase activity, then normalized to the activity of the p-491 MRP2-Luci construct transfected into cells. This result was representative of three experiments. $*P < .01$. MRP2, multidrug resistance protein 2.

To investigate whether an ERK inhibitor, PD98059, affects IL-1β-mediated suppression of *MRP2* promoter activity, we performed a transient transfection assay with p-491 MRP2-Luci and p-491(ISREmt) MRP2-Luci constructs in the presence or absence of this drug (Fig. 6). IL-1β again reduced the promoter activity of p-491 MRP2, and pretreatment with PD98059 significantly reduced IL-1β-mediated suppression of *MRP2* promoter activity. The basal promoter activity of p-491 (ISREmt) MRP2 was decreased relative to that of p-491 MRP2, and the suppression of the promoter activity of the mutant construct by IL-1β was not significant (Fig. 6). Coadministration of PD98059 seemed to have no effect on the p-491MRP2 (ISREmt)-driven luciferase activity.

Binding of IRF3 to ISRE on MRP2 Promoter is Reduced by IL-1β. EMSAs were performed to investigate the binding of IRF3 to *MRP2* promoter ISRE ele-

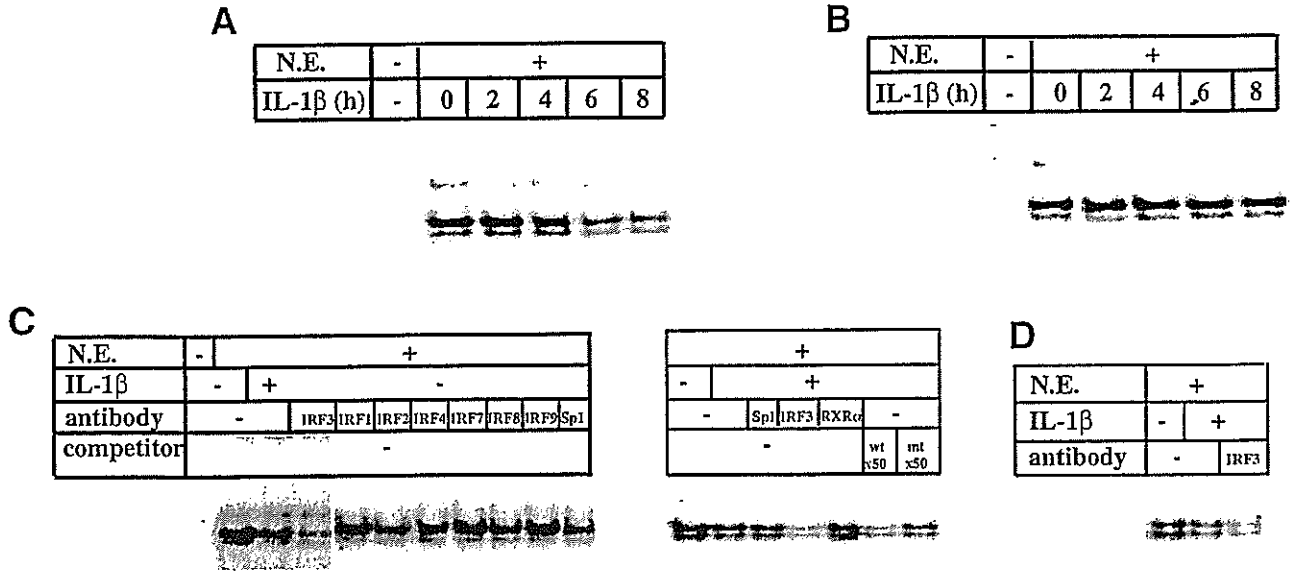

Fig. 7. Binding of IRF3 to *MRP2* promoter interferon stimulatory response elements (ISREs). Electrophoretic mobility shift assay (EMSA) was performed using radiolabeled probes, including interferon stimulatory response element (ISRE; −171/−159, 5′-GCAGCAGAAGCGAAACTGCAC-3′). For the competition assay, the unlabeled ISRE mutant probe (−179/−153: 5′-GCAGCAcgtGCGcgtCTGCA-3′) was used as a competitor. (A) Effects of interleukin-1β (IL-1β) on nuclear protein-ISRE binding. Cells were incubated with 20 ng/mL IL-1β for 0 to 8 hours. The nuclear extracts were prepared, and the extracts (4 μg of protein) that were incubated with ^{32}P-labeled oligonucleotide were resolved by gel electrophoresis. (B) Effects of PD98059 on IL-1β-induced *MRP2* downregulation. Before IL-1β stimulation, 20 μM PD98059 was administrated for 30 minutes. (C) Super shift and competition assay using nuclear extract with or without IL-1β for 8 hours. Anti-IRF1-4, 7-9, Sp1, and RXRα antibodies were added to the nuclear extracts. A 50-fold excess of the unlabeled oligonucleotide was added for the competition. (D) EMSA using nuclear extract from normal human hepatocytes (hNHeps). A bracket ([]) indicates the DNA protein complex. These results were representative of three experiments. IRF, interferon regulatory factor; RXR, retinoid X receptor; MRP2, multidrug resistance protein 2.

ments in nuclear extract from HepG2 cells. EMSA using radiolabeled ISRE oligonucleotides and nuclear extract showed two bands corresponding to specifically bound complexes (Fig. 7A). These ISRE–protein complex bands were reduced by treatment with 20 ng/mL IL-1β for 6 to 8 hours in the absence of an ERK inhibitor (Fig. 7A). By contrast, no decrease of ISRE–protein complex formation was observed when PD98059 was coadministered with IL-1β (Fig. 7B).

We next examined whether these diminished bands represented specific binding to ISRE and attempted to determine which protein was involved in the ISRE–protein complex formation. We used cold competitors and specific antibodies for IRF family members (Fig. 7C). A 50-fold excess of ISRE wild-type cold competitor was sufficient to abolish these bands. However, the retarded bands were not abolished when treated with mutant competitors (Fig. 7C), suggesting that the bands represented specific binding to the ISRE element. All members of the IRF family share homology in the DNA binding domain and bind to a similar DNA motif, the ISRE.[24,25] We performed supershift assays using antibodies of IRF family proteins IRF1, IRF2, IRF3, IRF4, IRF7, IRF8, and IRF9. As shown in Fig. 7C, the retarded bands were abolished specifically only when treated with anti-IRF3 antibody. Other IRF antibodies, Sp1 and RXR, retinoid X receptor (RXR) antibody, failed to shift these bands (Fig. 7C). This suggested that these two bands contain IRF3 protein–DNA complexes. IRF3 thus seemed to bind specifically to the ISRE element of the MRP2 promoter, and IRF3 binding activity to ISRE seemed to be reduced by treatment with IL-1β. We next examined whether nuclear extract from human primary hepatocytes instead of HepG2 could bind to ISRE elements. We observed that the specific ISRE–protein complex bands from human primary hepatocyte were reduced by treatment with IL-1β (Fig. 7D). We also observed that these retarded bands were abolished specifically when pretreated with anti-IRF3 antibody. These results suggested that human primary hepatocytes contain the IRF3 protein–DNA complexes.

Decreased IRF3 Translocation Into the Nucleus on Treatment With IL-1β. The reduction in IRF3 binding to ISRE could account for the observed IL-1β-mediated downregulation of *MRP2* mRNA expression. Reduced binding to ISRE could be caused by a lower expression of IRF3 at the protein level, or by the modification of IRF3 affecting DNA binding or nuclear import. We therefore investigated the expression of IRF3 after IL-1β treatment in the entire cell fraction (Fig. 8A, left), nuclear fraction

(Fig. 8A, middle), and cytoplasmic fraction of HepG2 cells (Fig. 8A, right). IRF3 is a phosphoprotein that is constitutively expressed in two forms of approximately 55 kD[26] in unstimulated HepG2 cells (Fig. 8A). The upper band of IRF3 could be basal IRF3 phosphorylation corresponding to the N-terminal of IRF3. In the nucleus, IRF3 protein abundance was reduced in this compartment when cells were treated with IL-1β for 8 hours. No reduction in cytoplasmic IRF3 protein and no change in the level of phosphorylation was observed when treated with IL-1β. High mobility group protein-I and glucose-6-phosphate dehydrogenase were used as markers for nuclear and cytoplasmic fraction, respectively. Pretreatment with PD98059 almost completely abolished the IL-1β-induced reduction of nuclear IRF3 protein level, even when cells were treated with IL-1β for 8 hours (Fig. 8B). IL-1β treatment did not change IRF3 protein levels in the whole cell fraction (Fig. 8A,B). To investigate the potential action of IRF3 on *MRP2* promoter activity, we used IRF3 expression vector fused Flag tags. The Flag-IRF3 or Flag-only vector was transiently cotransfected into HepG2 cells with a MRP2 promoter luciferase construct for 48 hours. Introduction of Flag-IRF3 from 20 to 200 ng induced an approximately 1.5- to 2.0-fold increase in wild-type *MRP2* promoter activity (Fig. 9). By contrast, no induction by Flag-IRF3 was observed when the ISRE mutant reporter was assayed. These results suggested that IRF3 may be involved in the basal transcriptional activity of the *MRP2* promoter through the ISRE element.

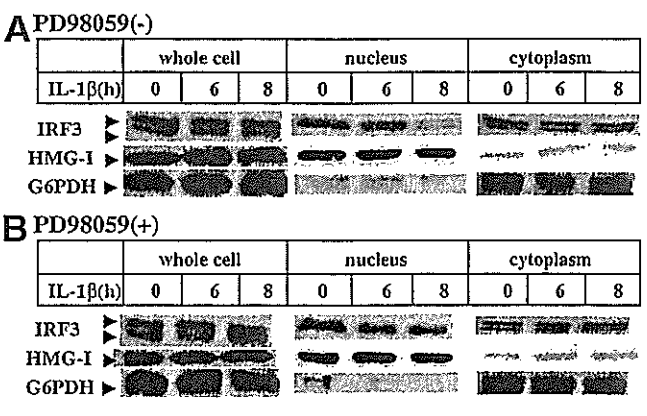

Fig. 8. Alteration of interferon regulatory factor 3 (IRF3) protein levels in HepG2 in response to interleukin-1β (IL-1β) administration with or without PD98059. 50 μg of whole cell lysate (**left panel**), 30 μg of nuclear extracts (**center**), and 50 μg of cytoplasmic extracts (**right**) were loaded onto each lane. (B) 20 μM PD98059 was administrated for 30 minutes before IL-1β stimulation. Anti-HMG-I antibodies and anti-glucose-6-phosphate dehydrogenase antibodies were used as nuclear and cytoplasmic protein controls. This result was representative of three experiments. HMG-I, high mobility group protein I.

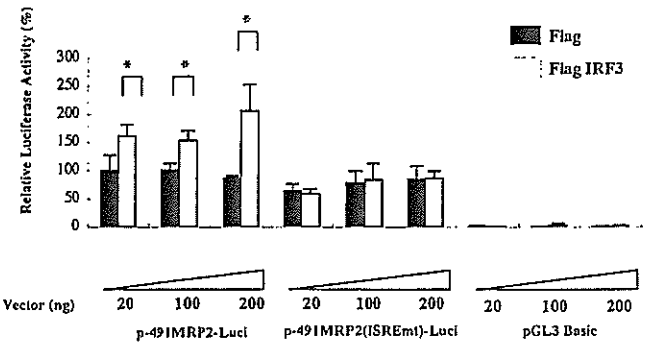

Fig. 9. Alteration of *MRP2* promoter-luciferase activity by expression of rIRF3 in HepG2 cells. Cells were transiently transfected with each construct, pRL-TK, and Flag or Flag-IRF3 for 24 hours and assayed for luciferase activity. Luciferase activities were corrected for differences in transfection efficiency by *Renilla* luciferase activity and were normalized to the activity of the pGL3 basic vector transfected into cells. Each dose of Flag or Flag-IRF3 was transiently transfected. This result was representative of three experiments. $*P < .01$. IRF3, interferon regulatory factor 3.

Discussion

Cholestasis and hyperbilirubinemia are common clinical features in various hepatic diseases, including virus-induced or drug-induced hepatitis, alcoholic hepatitis, sepsis, and idiopathic postoperative cholestasis.[27,28] Endotoxins and proinflammatory cytokines are thought to be among the main mediators of inflammation-induced cholestasis.[29,30] Recent studies have reported on the manner by which bile salts or cholesterol homeostasis-regulatory mechanisms are controlled through enterohepatic circulation at the molecular level. Altered expression levels of various transporters, including ABC transporters, have been implicated in cholestasis.[31] MRP2 is a typical canalicular ABC transporter that exports many essential organic anions. We previously characterized the 5′-flanking region of the human *MRP2* gene and its promoter activity in human hepatic cells.[4,20] Our subsequent study[19] demonstrated that *MRP2* promoter (p-2635)-driven luciferase activity in hepatic cells was greatly inhibited by IL-1β, and less so by TNFα or IL-6. Consistent with this study, our present study also indicates that *MRP2* promoter activity is highly susceptible to the inflammatory cytokine IL-1β. In this study, we demonstrate that treatment of HepG2 cells with IL-1β results in decreased levels of *MRP2* mRNA transcription. In addition, we demonstrate that a regulatory protein, IRF3, is responsible for the IL-1β-induced downregulation of *MRP2*. IRF3 activates the *MRP2* promoter through the ISRE under unstimulated conditions. Treatment with IL-1β induces a decrease in both nuclear accumulation of IRF3 and IRF3 binding to ISRE, resulting in downregulation of the *MRP2* gene.

Other incidences of IL-1β inducing downregulation of transporters have been reported recently. Denson et al.[32] reported that rat *ntcp* and *mrp2* genes are regulated by retinoic acid receptor:RXR, and that IL-1β reduces nuclear retinoic acid receptor:RXR. The retinoic acid receptor:RXR site is located in −210/−180 bp upstream from the transcription initiation site in the human *MRP2* promoter.

Our promoter deletion analysis and mutation of the promoter show that the IL-1β-induced inhibition of *MRP2* promoter activity is the result of the ISRE region downstream of retinoic acid receptor:RXR. It has also been reported that IL-1β-induced downregulation of the rat *ntcp* gene occurs via the JNK pathway,[33] whereas in our study, the downregulation of human *MRP2* by IL-1β occurs via the ERK pathway. Kast et al.[34] also reported that rat *mrp2* expression is regulated by the pregnane X receptor and constitutive androgen receptor, and that rat *mrp2* promoter activity is activated by nuclear receptor pregnane X receptor, constitutive androgen receptor, and their agonist. These results suggest that *MRP2* expression in the liver is regulated by environmental stimuli, numerous compounds through various nuclear receptors, and IRF3. The 5′-flanking region of the *MRP2* promoter contains C/EBPβ, HNF1, and USF elements, as well as an ISRE (Fig. 5).[20] Mutant constructs of ISRE and HNF show decreasing basal promoter activities when compared with the wild-type *MRP2* promoter, suggesting that these elements play a key role in the basal promoter activity. By contrast, there is an almost 3.0-fold increase in the promoter activity by a C/EBPβ mutation in the context of the *MRP2* promoter over wild type. Thus, C/EBPβ may regulate *MRP2* promoter activity negatively. We observed that IL-1β-induced suppression of *MRP2* mRNA is associated with the ISRE region of the *MRP2* promoter (Fig. 5). Among the various factors interacting with ISRE, IRF3 was found to bind specifically to the ISRE on the *MRP2* promoter (Fig. 7). EMSAs show two bands containing IRF3–protein complexes. These complexes may be the result of different proteins interacting with IRF3 or conformational changes within the protein. Expression of the exogenous IRF3 gene increases MRP2 promoter activity through the ISRE and when cells are treated with IL-1β levels of IRF3 in the nucleus are diminished (Fig. 8). IRF3 thus seems to be a positive transcription factor of the *MRP2* promoter in hepatic cells, and decreased levels of IRF3 in the nucleus may be responsible for IL-1β-induced downregulation of the *MRP2* promoter activity. However, we could not ruled out other transcription factor in IL-1β-mediated suppression of MRP2.

Infection of fibroblasts with human cytomegalovirus also causes nuclear translocation of IRF3 and cooperative DNA binding with the transcriptional coactivator CBP/p300.[35] On infection of a cell with a virus, the C-terminal domain of cytoplasmic IRF3 is phosphorylated and translocated to the nucleus of hematopoietic cells, where it activates several virus-induced genes.[26] Our work shows that IRF3 is expressed continuously in both the nucleus and cytoplasm of hepatic cells (Fig. 8). Uchiumi et al. (unpublished data). have demonstrated by immunohistochemical study that IRF3 is found to be localized mainly to the cytoplasm, with 10% of whole cell IRF3 in the nucleus. We observe a marked decrease in IRF3 protein levels in the nucleus accompanied by reduced formation of the IRF3–DNA complex when cells are treated with IL-1β for 6 hours or longer.

Coadministration of an ERK inhibitor (PD98059) relieves the suppression of *MRP2* mRNA expression and *MRP2* promoter activation by IL-1β and reverses the decreased binding of IRF3 to ISRE seen in the presence of IL-1β. IL-1β seems to decrease nuclear levels of a positive regulatory factor, IRF3, resulting in suppression of the *MRP2* promoter through the loss of interaction with ISRE. This process of IL-1β-induced suppression of the *MRP2* gene could be linked closely with ERK1/2 activation signaling.

In conclusion, among the many interferon regulatory factors, we determined that IRF3 has a specific interaction with ISRE on the *MRP2* promoter. The expression of exogenous IRF3 in hepatic cells activates reporter gene expression via the p-491MRP2 promoter construct containing wild-type ISRE, but not by p-491MRP2 (ISREmt) containing mutant ISRE. The expression levels of IRF3 in the nucleus decrease after cells are treated with IL-1β for 8 hours, concomitant with a reduction in the binding of IRF3 to ISRE at the MRP2 promoter.

References

1. Oude Elferink RP, Groen AK. The role of mdr2 P-glycoprotein in biliary lipid secretion. Cross-talk between cancer research and biliary physiology. J Hepatol 1995;23:617–625.
2. Elferink RO, Groen AK. Genetic defects in hepatobiliary transport. Biochim Biophys Acta 2002;1586:129–145.
3. Kuwano M, Uchiumi T, Hayakawa H, Ono M, Wada M, Izumi H, et al. The basic and clinical implications of ABC transporters, Y-box-binding protein-1 (YB-1) and angiogenesis-related factors in human malignancies. Cancer Sci 2003;94:9–14.
4. Taniguchi K, Wada M, Kohno K, Nakamura T, Kawabe T, Kawakami M, et al. A human canalicular multispecific organic anion transporter (cMOAT) gene is overexpressed in cisplatin-resistant human cancer cell lines with decreased drug accumulation. Cancer Res 1996;56:4124–4129.
5. Paulusma CC, Bosma PJ, Zaman GJ, Bakker CT, Otter M, Scheffer GL, et al. Congenital jaundice in rats with a mutation in a multidrug resistance-associated protein gene. Science 1996;271:1126–1128.
6. Suzuki H, Sugiyama Y. Single nucleotide polymorphisms in multidrug resistance associated protein 2 (MRP2/ABCC2): its impact on drug disposition. Adv Drug Deliv Rev 2002;54:1311–1331.

7. Paulusma CC, Kool M, Bosma PJ, Scheffer GL, ter Borg F, Scheper RJ, et al. A mutation in the human canalicular multispecific organic anion transporter gene causes the Dubin-Johnson syndrome. HEPATOLOGY 1997;25: 1539–1542.
8. Toh S, Wada M, Uchiumi T, Inokuchi A, Makino Y, Horie Y, et al. Genomic structure of the canalicular multispecific organic anion-transporter gene (MRP2/cMOAT) and mutations in the ATP-binding-cassette region in Dubin-Johnson syndrome. Am J Hum Genet 1999;64:739–746.
9. Wada M, Toh S, Taniguchi K, Nakamura T, Uchiumi T, Kohno K, et al. Mutations in the canilicular multispecific organic anion transporter (cMOAT) gene, a novel ABC transporter, in patients with hyperbilirubinemia II/Dubin-Johnson syndrome. Hum Mol Genet 1998;7:203–207.
10. Thorgeirsson SS, Huber BE, Sorrell S, Fojo A, Pastan I, Gottesman MM. Expression of the multidrug-resistant gene in hepatocarcinogenesis and regenerating rat liver. Science 1987;236:1120–1122.
11. Trauner M, Arrese M, Soroka CJ, Ananthanarayanan M, Koeppel TA, Schlosser SF, et al. The rat canalicular conjugate export pump (Mrp2) is down-regulated in intrahepatic and obstructive cholestasis. Gastroenterology 1997;113:255–264.
12. Vos TA, Hooiveld GJ, Koning H, Childs S, Meijer DK, Moshage H, et al. Up-regulation of the multidrug resistance genes, Mrp1 and Mdr1b, and down-regulation of the organic anion transporter, Mrp2, and the bile salt transporter, Spgp, in endotoxemic rat liver. HEPATOLOGY 1998;28:1637–1644.
13. Vos TA, Van Goor H, Tuyt L, De Jager-Krikken A, Leuvenink R, Kuipers F, et al. Expression of inducible nitric oxide synthase in endotoxemic rat hepatocytes is dependent on the cellular glutathione status. HEPATOLOGY 1999;29:421–426.
14. Gerloff T, Geier A, Stieger B, Hagenbuch B, Meier PJ, Matern S, et al. Differential expression of basolateral and canalicular organic anion transporters during regeneration of rat liver. Gastroenterology 1999;117:1408–1415.
15. Hartmann G, Cheung AK, Piquette-Miller M. Inflammatory cytokines, but not bile acids, regulate expression of murine hepatic anion transporters in endotoxemia. J Pharmacol Exp Ther 2002;303:273–281.
16. Genin P, Algarte M, Roof P, Lin R, Hiscott J. Regulation of RANTES chemokine gene expression requires cooperativity between NF-kappa B and IFN-regulatory factor transcription factors. J Immunol 2000;164: 5352–5361.
17. Barnes B, Lubyova B, Pitha PM. On the role of IRF in host defense. J Interferon Cytokine Res 2002;22:59–71.
18. Hiscott J, Pitha P, Genin P, Nguyen H, Heylbroeck C, Mamane Y, et al. Triggering the interferon response: the role of IRF-3 transcription factor. J Interferon Cytokine Res 1999;19:1–13.
19. Hinoshita E, Taguchi K, Inokuchi A, Uchiumi T, Kinukawa N, Shimada M, et al. Decreased expression of an ATP-binding cassette transporter, MRP2, in human livers with hepatitis C virus infection. J Hepatol 2001; 35:765–773.
20. Tanaka T, Uchiumi T, Hinoshita E, Inokuchi A, Toh S, Wada M, et al. The human multidrug resistance protein 2 gene: functional characterization of the 5′-flanking region and expression in hepatic cells. HEPATOLOGY 1999;30:1507–1512.
21. Inokuchi A, Hinoshita E, Iwamoto Y, Kohno K, Kuwano M, Uchiumi T. Enhanced expression of the human multidrug resistance protein 3 by bile salt in human enterocytes. A transcriptional control of a plausible bile acid transporter. J Biol Chem 2001;276:46822–46829.
22. Saklatvala J, Dean J, Finch A. Protein kinase cascades in intracellular signalling by interleukin-I and tumour necrosis factor. Biochem Soc Sympos 1999;64:63–77.
23. Moshage H. Cytokines and the hepatic acute phase response. J Pathol 1997;181:257–266.
24. Darnell JE Jr, Kerr IM, Stark GR. Jak-STAT pathways and transcriptional activation in response to IFNs and other extracellular signaling proteins. Science 1994;264:1415–1421.
25. Ihle JN, Kerr IM. Jaks and Stats in signaling by the cytokine receptor superfamily. Trends Genet 1995;11:69–74.
26. Servant MJ, Grandvaux N, Hiscott J. Multiple signaling pathways leading to the activation of interferon regulatory factor 3. Biochem Pharmacol 2002;64:985–992.
27. Trauner M, Fickert P, Stauber RE. Inflammation-induced cholestasis. J Gastroenterol Hepatol 1999;14:946–959.
28. Jansen PL, Roskams T. Why are patients with liver disease jaundiced? ATP-binding cassette transporter expression in human liver disease. J Hepatol 2001;35:811–813.
29. Trauner M, Arrese M, Lee H, Boyer JL, Karpen SJ. Endotoxin downregulates rat hepatic ntcp gene expression via decreased activity of critical transcription factors. J Clin Invest 1998;101:2092–2100.
30. Crawford JM, Boyer JL. Clinicopathology conferences: inflammation-induced cholestasis. HEPATOLOGY 1998;28:253–260.
31. Bolder U, Ton-Nu HT, Schteingart CD, Frick E, Hofmann AF. Hepatocyte transport of bile acids and organic anions in endotoxemic rats: impaired uptake and secretion. Gastroenterology 1997;112:214–225.
32. Denson LA, Auld KL, Schiek DS, McClure MH, Mangelsdorf DJ, Karpen SJ. Interleukin-1beta suppresses retinoid transactivation of two hepatic transporter genes involved in bile formation. J Biol Chem 2000;275:8835–8843.
33. Li D, Zimmerman TL, Thevananther S, Lee HY, Kurie JM, Karpen SJ. Interleukin-1 beta-mediated suppression of RXR:RAR transactivation of the Ntcp promoter is JNK-dependent. J Biol Chem 2002;277: 31416–31422.
34. Kast HR, Goodwin B, Tarr PT, Jones SA, Anisfeld AM, Stoltz CM, et al. Regulation of multidrug resistance-associated protein 2 (ABCC2) by the nuclear receptors pregnane X receptor, farnesoid X-activated receptor, and constitutive androstane receptor. J Biol Chem 2002;277:2908–2915.
35. Navarro L, Mowen K, Rodems S, Weaver B, Reich N, Spector D, et al. Cytomegalovirus activates interferon immediate-early response gene expression and an interferon regulatory factor 3-containing interferon-stimulated response element-binding complex. Mol Cell Biol 1998;18:3796–3802.

Direct inhibition of EGF receptor activation in vascular endothelial cells by gefitinib ('Iressa', ZD1839)

Akira Hirata,[1,2] Hisanori Uehara,[3] Keisuke Izumi,[3] Seiji Naito,[2] Michihiko Kuwano[4] and Mayumi Ono[1,5]

Departments of [1]Medical Biochemistry and [2]Urology, Graduate School of Medical Science, Kyushu University, 3-1-1 Maidashi, Higashi-ku, Fukuoka 812-8582; [3]Second Department of Pathology, The University of Tokushima School of Medicine, 2-50-1 Kuramotocho, Tokushima 770-0042; and [4]Research Center for Innovative Cancer Therapy of the 21st Century COE Program for Medical Science, Kurume University School of Medicine, 67 Asahimachi, Kurume 830-0011

(Received March 1, 2004/Revised May 8, 2004/Accepted May 24, 2004)

The development of gefitinib ('Iressa', ZD1839) by targeting the EGFR tyrosine kinase is a recent therapeutic highlight. We have reported that gefitinib is antiangiogenic *in vitro*, as well as *in vivo*. In this study, we asked if the anti-angiogenic action of gefitinib is due to a direct effect on activation of vascular endothelial cells by EGF. EGF, as well as VEGF, caused pronounced angiogenesis in an avascular area of the mouse cornea, and i.p. administration of gefitinib almost completely blocked the response to EGF, but not to VEGF. Immunohistochemical analysis demonstrated phosphorylation of EGFR by EGF in the neovasculature, and gefitinib markedly reduced this effect. Gefitinib also inhibited downstream activation of ERK 1/2 via EGFR in cultured microvascular endothelial (HMVE) cells. These findings suggest that the anti-angiogenic effect of gefitinib in the vascular endothelial cells of neo-vasculature is partly attributable to direct inhibition of EGFR activation, and that endothelial cells in malignant tumors play a critical role in the cancer therapeutic efficacy of gefitinib. (Cancer Sci 2004; 95: 614–618)

Protein tyrosine kinases play key roles in cell proliferation, cell death, development, differentiation, cell motility, morphogenesis, and angiogenesis.[1,2] The ErbB-family protein kinases are important representatives of this type of protein kinase, and their signaling network in development and differentiation has been well studied.[3,4] In particular, expression of the EGFR and other ErbB-family proteins is often associated with stimulation of cell growth and apoptosis in cancer. A recent therapeutic highlight is the development of targeted anticancer drugs, such as gefitinib ('Iressa', ZD1839) and herceptin, that inhibit ErbB-family tyrosine kinases.[5,6] Gefitinib is an orally active EGFR tyrosine kinase inhibitor that blocks signal transduction pathways implicated in cancer growth, and decreases cellular proliferation, angiogenesis, tumor invasion and metastasis while increasing apoptosis.[7–10] Gefitinib has anti-proliferation activity in various human cancer cell types *in vivo* as well as *in vitro*,[11,12] and is also effective in cancer patients.[7] Our recent study has demonstrated that sensitivity to gefitinib in non-small cell lung cancer cell lines is associated with dependence on Akt and ERK 1/2 activation in response to EGFR signaling.[13]

We have previously reported that gefitinib can inhibit angiogenesis *in vivo* as well as *in vitro*: it inhibited both EGF-induced migration of HMVE cells and EGF-induced neovascularization in the mouse cornea.[14] Angiogenesis is often provoked by the major pro-angiogenic factors, bFGF, VEGF, IL-8, PDGF, and EGF/TGFα.[15–17] The stimulatory effect of EGF/TGFα in angiogenesis is, however, not yet well understood. We have reported that EGF/TGFα-induced angiogenesis might be attributable to its signaling through direct interaction with vascular endothelial cells,[14,18] and also to angiogenesis-related factors that are produced from cancer cells and vascular endothelial cells, based on studies using various angiogenesis models.[14,19,20] However, it remains unclear whether EGF-induced angiogenesis *in vivo* is mediated by direct interaction with endothelial cells. The vascular endothelial cells in a number of tumor types are known to express EGFR,[21–23] and suppression of VEGF or EGF expression inhibited the growth of a wide variety of tumor types in a murine tumor model, while angiogenesis inhibitors that target VEGF receptor or EGFR reduced tumor growth, metastasis, and the microvessel density of human pancreatic cancer in nude mice.[24] In addition, blockade of EGFR by a tyrosine kinase inhibitor can suppress both EGFR-induced proliferation in cancer, and EGFR-induced survival of tumor-associated endothelial cells in an animal model.[25,26] The tyrosine kinase inhibitor also blocked activation of EGFR in tumor-associated endothelial cells. Taken together, these results indicate that EGFR is activated in response to EGF, TGFα, and other ligands that are secreted into the tumor microenvironment.

In the present study, we asked if gefitinib inhibits angiogenesis in vascular endothelial cells by interfering with EGFR activation, or by inhibiting the EGF/TGFα-induced expression of other potent angiogenic factors, such as VEGF and IL-8, as suggested by others.[27,28] We first present findings in the mouse cornea that point to direct involvement of EGF/EGFR signaling in angiogenesis by the vascular endothelial cells in EGF-induced neo-vasculature, and then present evidence that the anti-angiogenic effect of gefitinib is partly attributable to direct inhibition of EGFR activation in neo-vasculature by EGF.

Materials and Methods

Materials. Gefitinib was kindly provided by AstraZeneca (Macclesfield, UK). Murine EGF was purchased from Toyobo (Osaka, Japan) and recombinant mouse VEGF from R&D Systems, Inc. (Minneapolis, MN). Anti-EGFR antibody and anti-phospho-EGFR antibody were purchased from Upstate Biotechnology (Lake Placid, NY). Antibodies to ERK 1/2, phospho-ERK 1/2, Akt, and phospho-Akt were from Cell Signaling Technology (Beverly, MA).

Cell culture. HMVE cells derived from neonatal dermis (Cascade Biologics, Portland, OR) were cultured in medium 131 containing microvascular growth supplement (Cascade Biologics). We used cells at passage 3–4 after recovery from frozen stocks. The cells were maintained under standard cell culture conditions at 37°C and 5% CO_2 in a humid environment.

[5]To whom correspondence should be addressed.
E-mail: mayumi@biochem1.med.kyushu-u.ac.jp

Abbreviations: Akt, protein kinase B/Akt; bFGF, basic fibroblast growth factor; EGF, epidermal growth factor; EGFR, epidermal growth factor receptor; ERK, extracellular signal-regulated kinase; HMVE cells, human microvascular endothelial cells; IL-8, interleukin-8; TGFα, transforming growth factor α; VEGF, vascular endothelial growth factor.

'Iressa' is a trademark of the AstraZeneca group of companies.

Western blot analysis. HMVE cells were cultured in medium containing 1% FBS for 12 h, then incubated with 0 to 5 μ*M* gefitinib for 3 h before stimulation with 20 ng/ml EGF or 20 ng/ml VEGF for 10 min at 37°C. They were rinsed with ice-cold PBS then lysed in Triton X-100 buffer (50 μ*M* HEPES, 150 μ*M* NaCl, 1% Triton X-100 and 10% glycerol containing 1 m*M* PMSF, 10 μg/ml aprotinin, 10 μg/ml leupeptin and 1 m*M* sodium vanadate). Lysates were subjected to SDS polyacrylamide gel electrophoresis and transferred to Immobilon membranes (Millipore, Bedford, MA). Blots were incubated with blocking solution and probed with anti-EGFR antibody, anti-phospho-EGFR antibody, anti-ERK 1/2 antibody, anti-phospho-ERK 1/2 antibody, anti-Akt antibody and anti-phospho-Akt antibody, followed by washing. Antigen-antibody complexes were then visualized with horseradish peroxidase-conjugated secondary antibodies following by enhanced chemiluminescence (ECL; Amersham, Piscataway, NJ), as described previously.[14, 29]

Corneal micropocket assay in mice and quantification of corneal neo-vascularization. The corneal micropocket assay was performed essentially as previously described.[14, 30] Briefly, 0.3 μl of Hydron pellets (IFN Sciences, New Brunswick, NI) containing murine EGF (200 ng) or murine VEGF (200 ng) were implanted into the corneas of male BALB/c mice, and gefitinib was administered by i.p. injection (100 mg/kg/day) on days 1–5. On day 6, mice were sacrificed and their corneal vessels were photographed. Images of the corneas were recorded using Nikon Coolscan software with standardized illumination, contrast, and threshold settings, and were saved on disk. Areas of corneal neo-vascularization were analyzed using the software package NIH Image 1.61, and expressed in mm^2.

Immunofluorescence double staining for CD31/PECAM-1 and EGFR or phospho-EGFR (Tyr845). Frozen sections were fixed in cold acetone for 10 min. After having been rinsed three times for 3 min each with PBS, sections that had been immunostained for CD31/EGF-R and CD31/phospho-EGFR were incubated with a 1:100 dilution of monoclonal rat anti-mouse CD31/PECAM-1 antibody (PharMingen, San Diego, CA) containing 5% normal goat serum for 1 h at room temperature. The sections were rinsed again three times for 3 min each with PBS, then incubated with a 1:400 dilution of secondary Alexa 594-conjugated goat anti-rat IgG antibody (Molecular Probes, Eugene, OR) for 1 h at room temperature in the dark. Samples were then rinsed three times with PBS, and incubated at 4°C for 18 h with a 1:50 dilution of polyclonal rabbit anti-human EGFR antibody (Santa Cruz Biotechnology, Santa Cruz, CA) and a 1:50 dilution of polyclonal rabbit anti-phospho-EGFR (Tyr845) antibody (Cell Signaling Technology), both of which are mouse cross-reactive. The samples were further rinsed three times for 3 min each with PBS, then incubated with a 1:400 dilution of secondary Alexa 488-conjugated goat anti-rabbit IgG (Molecular Probes) for 1 h at room temperature in the dark. The samples were then rinsed three times for 5 min each with PBS and mounted with Vectashield (Vector Laboratories, Inc., Burlingame, CA). Immunofluorescence microscopy was performed using a ×20 objective. The images were captured using a CoolSNAP camera, Epifluorescence upright microscopy system (Olympus Optical Co., Ltd., Tokyo), and MetaCam software (Universal Imaging Corporation, Downingtown, PA).

Statistical analysis. Statistical comparisons were performed using the Mann-Whitney test; $P<0.05$ was considered significant.

Results

Gefitinib inhibits EGF-induced angiogenesis but not VEGF-induced angiogenesis. We first examined if EGF or VEGF could induce angiogenesis in the mouse cornea. Administration of EGF or VEGF in Hydron pellets induced marked angiogenesis in an avascular area of the cornea (Fig. 1, A and C), consistent with our previous study.[14] I.p. administration of gefitinib blocked EGF-induced neo-vascularization, but not VEGF-induced neo-vascularization. Quantitative analysis using four mice in each assay consistently showed more than 70% inhibition of EGF-induced neo-vascularization by gefitinib, and almost no inhibition of VEGF-induced neo-vascularization (Fig. 1B).

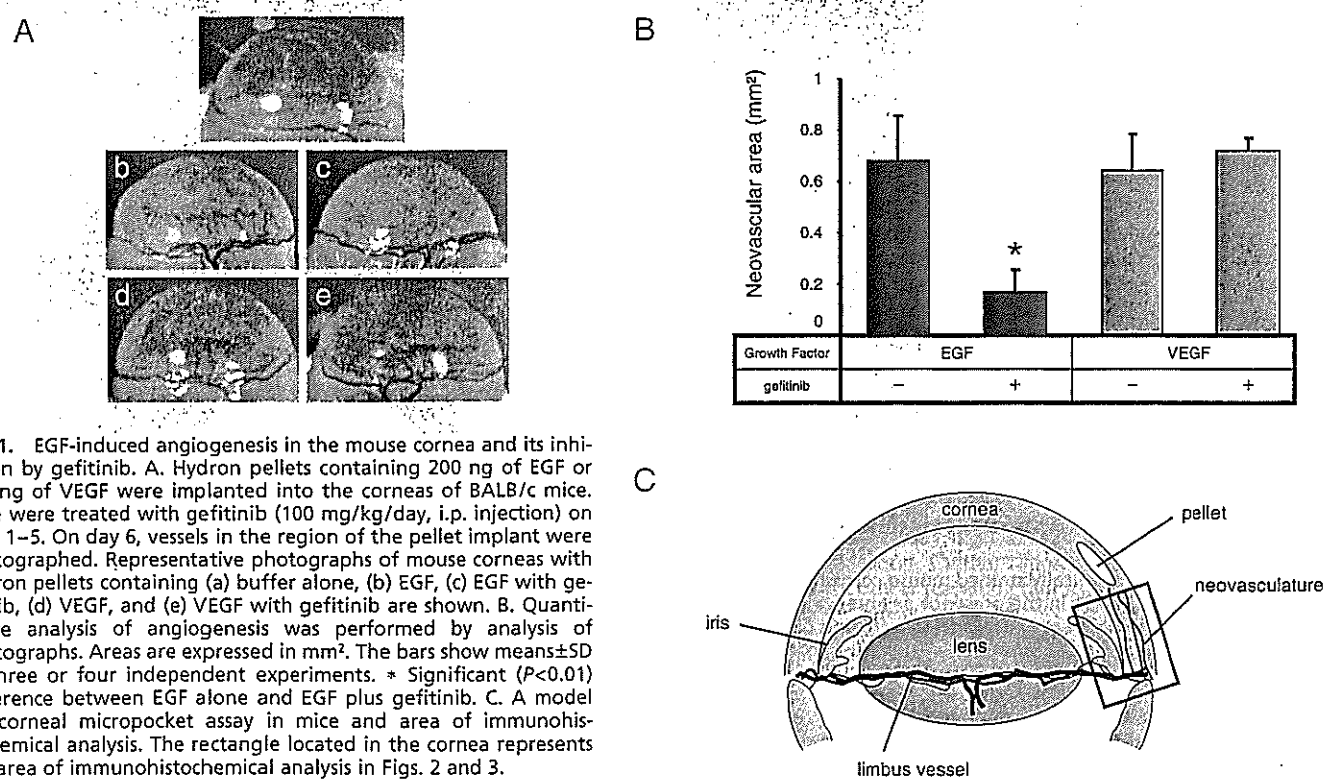

Fig. 1. EGF-induced angiogenesis in the mouse cornea and its inhibition by gefitinib. A. Hydron pellets containing 200 ng of EGF or 200 ng of VEGF were implanted into the corneas of BALB/c mice. Mice were treated with gefitinib (100 mg/kg/day, i.p. injection) on days 1–5. On day 6, vessels in the region of the pellet implant were photographed. Representative photographs of mouse corneas with Hydron pellets containing (a) buffer alone, (b) EGF, (c) EGF with gefitinib, (d) VEGF, and (e) VEGF with gefitinib are shown. B. Quantitative analysis of angiogenesis was performed by analysis of photographs. Areas are expressed in mm^2. The bars show means±SD of three or four independent experiments. * Significant ($P<0.01$) difference between EGF alone and EGF plus gefitinib. C. A model for corneal micropocket assay in mice and area of immunohistochemical analysis. The rectangle located in the cornea represents the area of immunohistochemical analysis in Figs. 2 and 3.

Gefitinib inhibits EGF-induced EGFR activation in EGF-induced neovasculature. To determine whether gefitinib inhibits EGFR phosphorylation in endothelial cells, we performed an immunohistochemical analysis of the corneal micropocket of mice. Cross sections of cornea exposed to EGF or VEGF in the area exhibited in Fig. 1C showed the development of extensive CD31-positive neo-vasculature (Fig. 2). Some EGFR-positive cells were observed in the CD31-positive vascular endothelial cells in corneas induced by EGF or VEGF whether or not gefitinib was present (Fig. 2). However, the number of EGFR-positive vascular endothelial cells in vasculature induced by VEGF was somewhat smaller than that in the case of EGF. By contrast, there were few, if any, EGFR-positive cells in the control untreated group.

We next examined whether the EGFR in the EGF-induced corneal neo-vasculatures was phosphorylated. To our surprise, we found many endothelial cells in neo-vasculature induced by EGF, but not that induced by VEGF, stained positively for phosphorylated EGFR (Fig. 3). More than 50% of endothelial cells were phospho-EGFR positive. Daily i.p. administration of gefitinib resulted in reduced numbers of phospho-EGFR-positive cells with a concomitant decrease in corneal angiogenesis (Fig. 3). Gefitinib however did not affect the development of neo-vasculature, or the phosphorylation state of EGFR, in response to VEGF.

Gefitinib inhibits EGF-induced, but not VEGF-induced activation of ERK 1/2 *in vitro*. We previously reported that EGFR phosphorylation and EGF-activated signaling were inhibited by gefitinib in EGFR-expressing HMVE cells derived from human omentum.[14] In our present study, we examined if EGF/EGFR signaling was activated in another type of HMVE cells derived from neonatal dermis with very low levels of EGFR. Both Akt and ERK 1/2 were phosphorylated by EGF in these HMVE cells (Fig. 4A). Moreover, gefitinib at 0.1 μM almost completely inhibited EGF-induced activation of ERK 1/2, while at 5 μM it reduced Akt phosphorylation to the untreated control level (Fig.

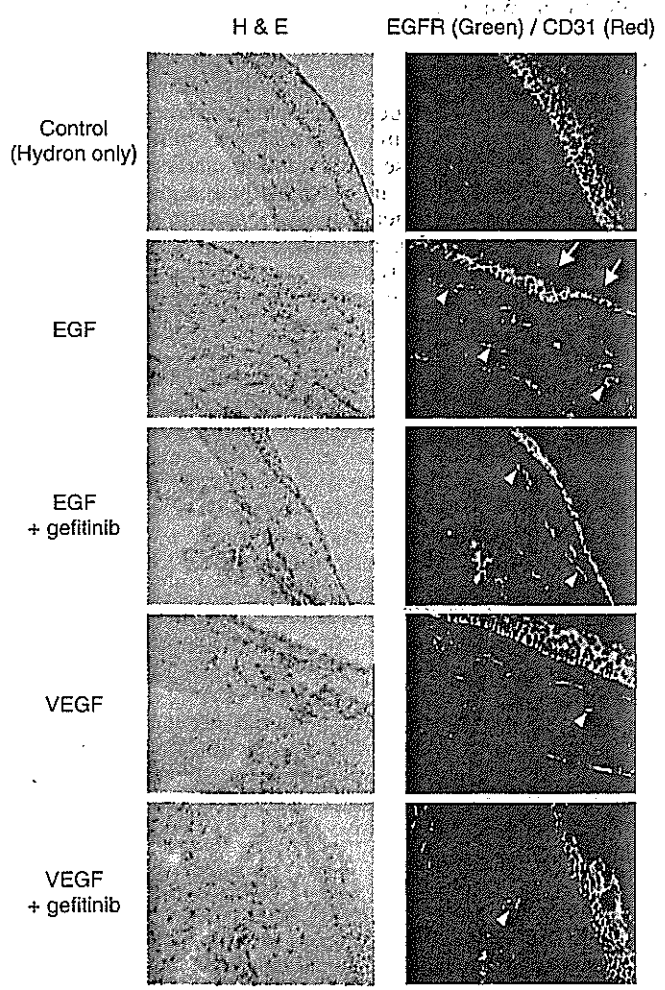

Fig. 2. Immunohistochemically stained mouse cornea sections and expression of EGFR and CD31 in the presence or absence of EGF or VEGF with or without gefitinib treatment. EGFR (green) and CD31 (red) were immunostained with specific antibodies in mouse cornea sections. CD31-positive cells are indicative of EGF or VEGF-induced neo-vasculature in the cornea. Hematoxylin-eosin (H&E) staining of counterparts of each stained sample is shown in the left panel. In the photograph of cornea exposed to EGF: white arrow, epithelial layer in cornea; white arrowhead, neo-vasculature in corneal stromal layer. ×400.

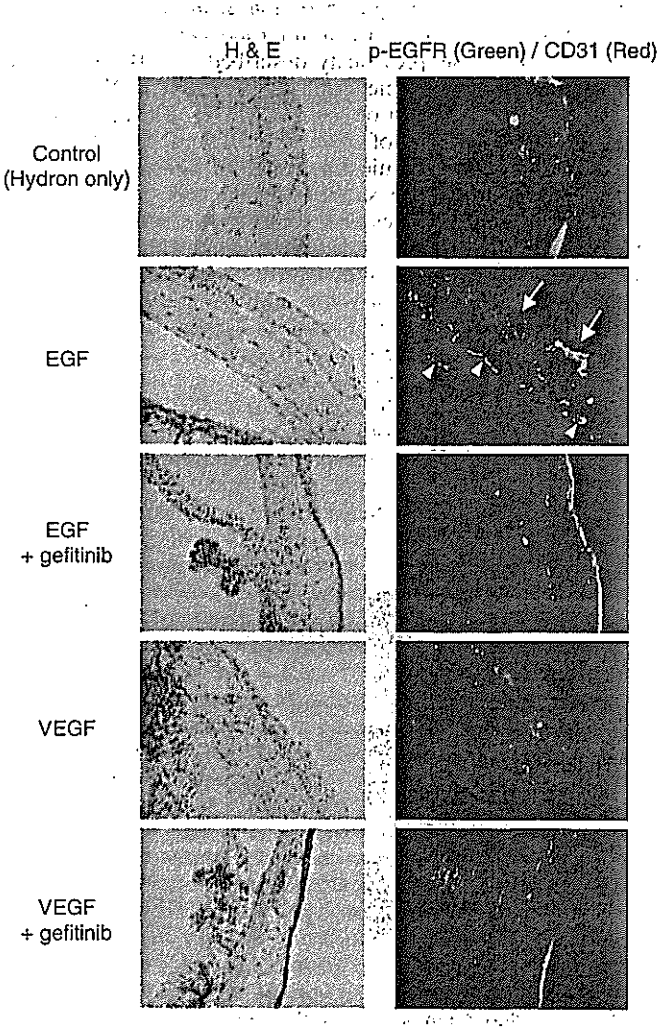

Fig. 3. EGF-induced EGFR phosphorylation of neo-vasculature in mouse corneas and inhibition by gefitinib. Immunohistochemical analysis was performed on mouse cornea sections with specific antibodies against CD31 (red) and phosphorylated EGFR (green). Many endothelial cells in the neo-vasculature are positive for phosphorylated EGFR (merged, yellow) after stimulation with EGF, and i.p. administration of gefitinib diminishes the appearance of such phosphorylated EGFR-positive cells. In contrast, almost no cells positive for phosphorylated EGFR were observed in neo-vasculature formed in response to VEGF with or without administration of gefitinib. Hematoxylin-eosin (H&E) staining of counterparts of each stained sample is shown in the left panel. In the photograph of cornea exposed to EGF: white arrow, epithelial layer in cornea; white arrowhead, neovasculature in corneal stromal layer. ×400.

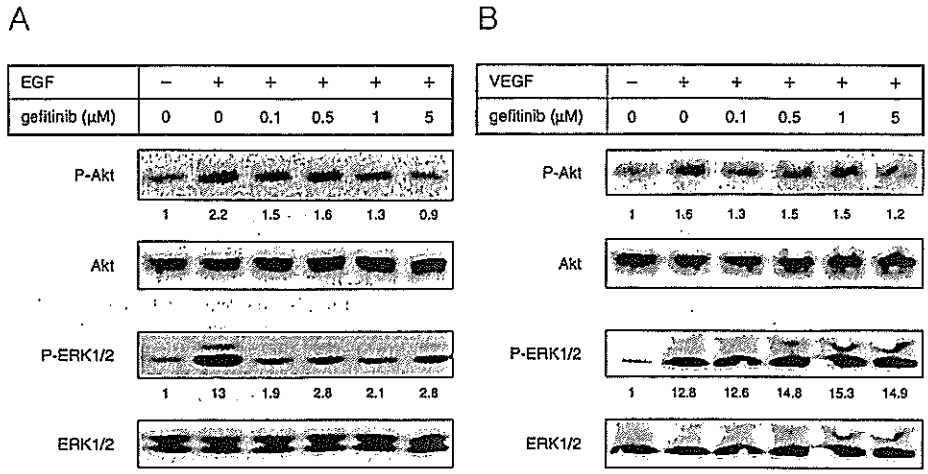

Fig. 4. Inhibition of EGF-induced but not VEGF-induced activation of Akt and ERK 1/2 by gefitinib in HMVE cells. Serum-starved HMVE cells were treated for 3 h with gefitinib, followed by (A) EGF (20 ng/ml) or (B) VEGF (20 ng/ml) for 10 min. Protein extracts were resolved by SDS-PAGE and probed with specific antibodies. Akt and ERK 1/2 activities were determined with anti-phospho-Akt and anti-phospho-ERK 1/2 antibodies, and the immunoreactive proteins were visualized by means of enhanced chemiluminescence. Activities of phosphorylated Akt and ERK 1/2 are normalized to their activities in the absence of EGF or VEGF.

4A). We could detect a small amount of EGFR in these cells by western blot analysis, but failed to detect any phosphorylation of EGFR with antibody against phosphorylated EGFR (data not shown). As shown in Fig. 4B, both Akt and ERK 1/2 were also activated by VEGF in HMVE cells. However, gefitinib could not inhibit this activation by VEGF.

Discussion

We have shown that EGF is as potent as VEGF in inducing angiogenesis in a mouse cornea assay, in agreement with our previous study.[14] Both indirect and direct mechanisms have been considered to underlie EGF/TGFα-induced angiogenesis: on the one hand, EGF/TGFα secreted by tumor cells and/or tumor stoma cells enhanced the production of potent angiogenic factors, such as VEGF, IL-8, and metalloproteinases, resulting in angiogenesis via the paracrine and/or autocrine route[31–33]; on the other hand, activation of EGFR expressed in neo-vasculature in response to EGF/TGFα induced an angiogenic switch of the endothelial cells.[18, 20, 22] Concerning the latter direct mechanism, some dividing endothelial cells have been shown to express EGFR.[21, 23, 34] In addition, Fidler and colleagues have recently reported that tumor-associated endothelial cells express activated EGFR, and also that administration of EGFR tyrosine kinase inhibitors decreases this EGFR activation, with concomitant inhibition of tumor growth and/or metastasis and induction of apoptosis of the endothelial cells.[25, 26, 35] We also demonstrated above a marked decrease in the number of vascular endothelial cells with phosphorylated EGFR in response to gefitinib. In contrast, gefitinib had almost no effect on VEGF-induced neo-vascularization. We may therefore conclude that, in the present *in vivo* model, activated EGFR is directly involved in angiogenesis in response to EGF. In agreement with this notion, we also observed that gefitinib inhibits downstream activation of ERK 1/2 by EGF/EGFR *in vitro* (see Fig. 4A).

Activation of MAPK and Akt in vascular endothelial cells appears to be essential for angiogenesis. Kim *et al.*[36] have reported that betacellulin, a member of the EGF family, has an angiogenic effect in the Matrigel plug assay, and that it activates ERK 1/2 and Akt in human umbilical vascular endothelial cells. We have also shown that EGF activates MAPK and Akt in HMVE cells derived from neonatal dermis *in vitro* (this study) as well as in HMVE cells derived from the omentum.[14] Gefitinib caused rather more inhibition of the activation of ERK 1/2 than of Akt, and it is possible that activation of ERK 1/2 in vascular endothelial cells is more closely associated with the EGF-induced angiogenesis switch than is activation of Akt. However, this matter needs further clarification.

Both EGF and EGFR are expressed in the corneal epithelium,[37] and systemic administration of gefitinib not only delayed the healing of a corneal epithelial wound, but also reduced the thickness of unwounded corneal epithelium.[38] This suggests that EGFR plays a key role in corneal wound healing and homeostasis of the corneal epithelium. We also observed expression of EGFR, and its activation, in the corneal epithelium (Figs. 2 and 3). Whereas activation of EGFR in the neovasculature of the corneal stroma was highly susceptible to inhibition of gefitinib, activation of EGFR in the corneal epithelium appeared to be resistant. It may be that EGF/EGFR levels and activation of EGFR are not responsive to environmental stimuli and poisons in the corneal epithelium. Alternatively, the corneal epithelium may possess homeostatic mechanisms of the kind demonstrated by Wilson *et al.*,[39] or be protected by the corneal blood-epithelium barrier.

In conclusion, EGF/TGFα and related ligands are produced by many types of tumors. The antitumor effect of gefitinib and other EGFR tyrosine kinase inhibitors appears to be partly attributable to their anti-angiogenic activities via direct inhibition of EGFR activation in neo-vasculature in response to these ligands.

This study was supported by a grant-in-aid for cancer research from the Ministry of Education, Culture, Sports, Science and Technology, Japan, and also by a cancer research grant from the Ministry of Health, Labour and Welfare, Japan.

1. Ullrich A, Schlessinger J. Signal transduction by receptors with tyrosine kinase activity. *Cell* 1990; 61: 203–12.
2. Yarden Y, Ullrich A. Growth factor receptor tyrosine kinases. *Annu Rev Biochem* 1988; 57: 443–78.
3. Olayioye MA, Neve RM, Lane HA, Hynes NE. The ErbB signaling network: receptor heterodimerization in development and cancer. *EMBO J* 2000; 19: 3159–67.
4. Prenzel N, Fischer OM, Streit S, Hart S, Ullrich A. The epidermal growth factor receptor family as a central element for cellular signal transduction and diversification. *Endocr Relat Cancer* 2001; 8: 11–31.

5. Baselga J. Why the epidermal growth factor receptor? The rationale for cancer therapy. *Oncologist* 2002; 7 Suppl 4: 2–8.
6. Mendelsohn J, Baselga J. The EGF receptor family as targets for cancer therapy. *Oncogene* 2000; 19: 6550–65.
7. Baselga J, Averbuch SD. ZD1839 ('Iressa') as an anticancer agent. *Drugs* 2000; 60 Suppl 1: 33–40; discussion 41-32.
8. Barker AJ, Gibson KH, Grundy W, Godfrey AA, Barlow JJ, Healy MP, Woodburn JR, Ashton SE, Curry BJ, Scarlett L, Henthorn L, Richards L. Studies leading to the identification of ZD1839 (IRESSA): an orally active, selective epidermal growth factor receptor tyrosine kinase inhibitor targeted to the treatment of cancer. *Bioorg Med Chem Lett* 2001; 11: 1911–4.
9. Arteaga CL, Johnson DH. Tyrosine kinase inhibitors—ZD1839 (Iressa). *Curr Opin Oncol* 2001; 13: 491–8.
10. Woodburn JR. The epidermal growth factor receptor and its inhibition in cancer therapy. *Pharmacol Ther* 1999; 82: 241–50.
11. Ciardiello F, Caputo R, Bianco R, Damiano V, Pomatico G, De Placido S, Bianco AR, Tortora G. Antitumor effect and potentiation of cytotoxic drugs activity in human cancer cells by ZD-1839 (Iressa), an epidermal growth factor receptor-selective tyrosine kinase inhibitor. *Clin Cancer Res* 2000; 6: 2053–63.
12. Sirotnak FM, Zakowski MF, Miller VA, Scher HI, Kris MG. Efficacy of cytotoxic agents against human tumor xenografts is markedly enhanced by coadministration of ZD1839 (Iressa), an inhibitor of EGFR tyrosine kinase. *Clin Cancer Res* 2000; 6: 4885–92.
13. Ono M, Hirata A, Kometani T, Miyagawa M, Ueda S, Kinoshita H, Fujii T, Kuwano M. Sensitivity to gefitinib (Iressa, ZD1839) in non-small cell lung cancer cell lines correlates with dependence on the EGF receptor/ERK1/2 and EGF receptor/Akt pathway for proliferation. *Mol Cancer Ther* 2004; 3: 465–72.
14. Hirata A, Ogawa S, Kometani T, Kuwano T, Naito S, Kuwano M, Ono M. ZD1839 (Iressa) induces antiangiogenic effects through inhibition of epidermal growth factor receptor tyrosine kinase. *Cancer Res* 2002; 62: 2554–60.
15. Klagsbrun M, D'Amore PA. Regulators of angiogenesis. *Annu Rev Physiol* 1991; 53: 217–39.
16. Hanahan D, Folkman J. Patterns and emerging mechanisms of the angiogenic switch during tumorigenesis. *Cell* 1996; 86: 353–64.
17. Kuwano M, Fukushi J, Okamoto M, Nishie A, Goto H, Ishibashi T, Ono M. Angiogenesis factors. *Intern Med* 2001; 40: 565–72.
18. Ono M, Okamura K, Nakayama Y, Tomita M, Sato Y, Komatsu Y, Kuwano M. Induction of human microvascular endothelial tubular morphogenesis by human keratinocytes: involvement of transforming growth factor-alpha. *Biochem Biophys Res Commun* 1992; 189: 601–9.
19. Sato Y, Okamura K, Morimoto A, Hamanaka R, Hamaguchi K, Shimada T, Ono M, Kohno K, Sakata T, Kuwano M. Indispensable role of tissue-type plasminogen activator in growth factor-dependent tube formation of human microvascular endothelial cells *in vitro*. *Exp Cell Res* 1993; 204: 223–9.
20. Mawatari M, Okamura K, Matsuda T, Hamanaka R, Mizoguchi H, Higashio K, Kohno K, Kuwano M. Tumor necrosis factor and epidermal growth factor modulate migration of human microvascular endothelial cells and production of tissue-type plasminogen activator and its inhibitor. *Exp Cell Res* 1991; 192: 574–80.
21. Schreiber AB, Winkler ME, Derynck R. Transforming growth factor-alpha: a more potent angiogenic mediator than epidermal growth factor. *Science* 1986; 232: 1250–3.
22. Goldman CK, Kim J, Wong WL, King V, Brock T, Gillespie GY. Epidermal growth factor stimulates vascular endothelial growth factor production by human malignant glioma cells: a model of glioblastoma multiforme pathophysiology. *Mol Biol Cell* 1993; 4: 121–33.
23. Rockwell P, O'Connor WJ, King K, Goldstein NI, Zhang LM, Stein CA. Cell-surface perturbations of the epidermal growth factor and vascular endothelial growth factor receptors by phosphorothioate oligodeoxynucleotides. *Proc Natl Acad Sci USA* 1997; 94: 6523–8.
24. Baker CH, Solorzano CC, Fidler IJ. Blockade of vascular endothelial growth factor receptor and epidermal growth factor receptor signaling for therapy of metastatic human pancreatic cancer. *Cancer Res* 2002; 62: 1996–2003.
25. Baker CH, Kedar D, McCarty MF, Tsan R, Weber KL, Bucana CD, Fidler IJ. Blockade of epidermal growth factor receptor signaling on tumor cells and tumor-associated endothelial cells for therapy of human carcinomas. *Am J Pathol* 2002; 161: 929–38.
26. Kim SJ, Uehara H, Karashima T, Shepherd DL, Killion JJ, Fidler IJ. Blockade of epidermal growth factor receptor signaling in tumor cells and tumor-associated endothelial cells for therapy of androgen-independent human prostate cancer growing in the bone of nude mice. *Clin Cancer Res* 2003; 9: 1200–10.
27. Kerbel RS, Viloria-Petit A, Okada F, Rak J. Establishing a link between oncogenes and tumor angiogenesis. *Mol Med* 1998; 4: 286–95.
28. de Jong JS, van Diest PJ, van der Valk P, Baak JP. Expression of growth factors, growth-inhibiting factors, and their receptors in invasive breast cancer. II: Correlations with proliferation and angiogenesis. *J Pathol* 1998; 184: 53–7.
29. Nakao S, Kuwano T, Ishibashi T, Kuwano M, Ono M. Synergistic effect of TNF-alpha in soluble VCAM-1-induced angiogenesis through alpha(4) integrins. *J Immunol* 2003; 170: 5704–11.
30. Gimbrone MA Jr, Gullino PM. Neovascularization induced by intraocular xenografts of normal, preneoplastic, and neoplastic mouse mammary tissues. *J Natl Cancer Inst* 1976; 56: 305–18.
31. Benjamin LE, Keshet E. Conditional switching of vascular endothelial growth factor (VEGF) expression in tumors: induction of endothelial cell shedding and regression of hemangioblastoma-like vessels by VEGF withdrawal. *Proc Natl Acad Sci USA* 1997; 94: 8761–6.
32. Kitadai Y, Haruma K, Sumii K, Yamamoto S, Ue T, Yokozaki H, Yasui W, Ohmoto Y, Kajiyama G, Fidler IJ, Tahara E. Expression of interleukin-8 correlates with vascularity in human gastric carcinomas. *Am J Pathol* 1998; 152: 93–100.
33. Bancroft CC, Chen Z, Yeh J, Sunwoo JB, Yeh NT, Jackson S, Jackson C, Van Waes C. Effects of pharmacologic antagonists of epidermal growth factor receptor, PI3K and MEK signal kinases on NF-kappaB and AP-1 activation and IL-8 and VEGF expression in human head and neck squamous cell carcinoma lines. *Int J Cancer* 2002; 99: 538–48.
34. Bohling T, Hatva E, Kujala M, Claesson-Welsh L, Alitalo K, Haltia M. Expression of growth factors and growth factor receptors in capillary hemangioblastoma. *J Neuropathol Exp Neurol* 1996; 55: 522–7.
35. Bruns CJ, Solorzano CC, Harbison MT, Ozawa S, Tsan R, Fan D, Abbruzzese J, Traxler P, Buchdunger E, Radinsky R, Fidler IJ. Blockade of the epidermal growth factor receptor signaling by a novel tyrosine kinase inhibitor leads to apoptosis of endothelial cells and therapy of human pancreatic carcinoma. *Cancer Res* 2000; 60: 2926–35.
36. Kim HS, Shin HS, Kwak HJ, Cho CH, Lee CO, Koh GY. Betacellulin induces angiogenesis through activation of mitogen-activated protein kinase and phosphatidylinositol 3'-kinase in endothelial cell. *FASEB J* 2003; 17: 318–20.
37. Wilson SE, Schultz GS, Chegini N, Weng J, He YG. Epidermal growth factor, transforming growth factor alpha, transforming growth factor beta, acidic fibroblast growth factor, basic fibroblast growth factor, and interleukin-1 proteins in the cornea. *Exp Eye Res* 1994; 59: 63–71.
38. Nakamura Y, Sotozono C, Kinoshita S. The epidermal growth factor receptor (EGFR): role in corneal wound healing and homeostasis. *Exp Eye Res* 2001; 72: 511–7.
39. Wilson SE, Chen L, Mohan RR, Liang Q, Liu J. Expression of HGF, KGF, EGF and receptor messenger RNAs following corneal epithelial wounding. *Exp Eye Res* 1999; 68: 377–97.

GLIA 47:325–334 (2004)

N-myc Downstream-Regulated Gene 1 Expression in Injured Sciatic Nerves

KAZUHO HIRATA,[1]* KATSUAKI MASUDA,[2] WATARU MORIKAWA,[2] JIAN-WEN HE,[1] AKIO KURAOKA,[1] MICHIHIKO KUWANO,[2] AND MASARU KAWABUCHI[1]
[1]*Department of Anatomy and Cell Biology, Graduate School of Medical Sciences, Kyushu University, Fukuoka, Japan*
[2]*Department of Medical Biochemistry, Graduate School of Medical Sciences, Kyushu University, Fukuoka, Japan*

KEY WORDS NDRG1; nerve regeneration; Schwann cells; immunohistochemistry

ABSTRACT N-myc downstream-regulated gene 1 (NDRG1)/RTP/Drg1/Cap43/rit42/TDD5/Ndr1 is expressed ubiquitously and has been proposed to play a role in growth arrest and cell differentiation. A recent study showed that mutation of this gene is responsible for hereditary motor and sensory neuropathy-Lom. However, the role of this gene in the peripheral nervous system is not fully understood. In our study, rabbit polyclonal antibodies were raised against this gene product and were used to examine changes in its expression over the time course of Wallerian degeneration and ensuing regeneration after crush injury of mouse sciatic nerves. Fluorescent immunohistochemistry showed that NDRG1 was expressed over the intact nerve fibers. Double labeling with a Schwann cell (SC) marker, S-100 protein (S-100), revealed that NDRG1 was localized in the cytoplasm of S-100-positive Schwann cells (SCs). NDRG1 expression was maintained in the early stage of myelin degradation but was then markedly depleted at the end stage of myelin degradation when frequent occurrence of BrdU-labeled SCs was observed (at 7–9 days). The depletion of NDRG1 at this time point was also confirmed by Western blotting analysis. NDRG1 expression finally recovered at the stage of remyelination, with immunoreactivity stronger than that in intact nerves. These findings suggest that NDRG1 may play an important role in the terminal differentiation of SCs during nerve regeneration.

INTRODUCTION

N-myc downstream-regulated gene 1 was originally designated reducing agent and tunicamycin-responsive protein (RTP) (Kokame et al., 1996), homologues of which were then isolated repeatedly: human differentiation-related gene 1 (Drg1) (van Belzen et al., 1997), human protein induced by free intracellular Ca^{2+} (Cap43) (Zhou et al., 1998), the mouse homologue designated TDD5 (Lin and Chang, 1997), reduced in tumor, p43 (rit42) (Kurdistani et al., 1998), and N-myc-downstream, repressed gene 1 (Ndr1) (Shimono et al., 1999). Currently the official name of this gene is NDRG1, determined by the HUGO Gene Nomenclature Committee (Qu et al., 2002). We have adopted the nomenclature NDRG1 in this report. A recent study showed that NDRG1 is a member of the NDRG gene family that contains an α/-β-hydrolase fold (Qu et al., 2002) without the residues required for catalysis (Shaw et al., 2002). It encodes a highly conserved protein with a high degree of homology to the proteins in other species, such as zebrafish (Gen Bank Accession Nos. AW281236 and AI657643), fruit flies (AF145604 and AE003454), nematodes (Z68135 and AL132847), sunflowers (Y09057 and AF189147) (Krauter-Canham et al., 1997), and *Arabidopsis* (AC005917 and AL163814). The evolutional conservation of this gene implies that it plays an important biological role. This gene has been reported to be involved in cell growth and differ-

*Correspondence to: Kazuho Hirata, Department of Anatomy and Cell Biology, Graduate School of Medical Sciences, Kyushu University, Higashi-ku, Maidashi 3-1-1, Fukuoka, 812-8582 Japan. E-mail: hirata@anat1.med.kyushu-u.ac.jp

Received 20 September 2003; Accepted 29 January 2004
DOI 10.1002/glia.20037
Published online 30 April 2004 in Wiley InterScience (www.interscience.wiley.com).